ACS APPLIED ELECTRONIC MATERIALS

pubs.acs.org/acsaelm Forum Article

Future Trends in Alternative Sustainable Materials for Low-Temperature Thermoelectric Applications

Víctor Toral, Sonia Gómez-Gijón, Francisco J. Romero, Diego P. Morales, Encarnación Castillo, Noel Rodríguez, Sara Rojas, Francisco Molina-Lopez,* and Almudena Rivadeneyra*

Cite This: https://doi.org/10.1021/acsaelm.4c00770 Read Online

ACCESS | Metrics & More | Article Recommendations

ABSTRACT: In the evolution of pervasive electronics, it is imperative to significantly reduce the energy consumption of power systems and embrace sustainable materials and fabrication processes with minimal carbon footprint. Within this context, thermoelectric generators (TEGs) have garnered substantial attention in recent years because of the readily available thermal gradients in the environment, making them a promising energy-harvesting technology. Current commercial room-temperature thermoelectrics are based on scarce, expensive, and/or toxic V−VI chalcogenide materials, which limit their widespread use. Thermoelectric polymers partially address this issue, and as such, they have been intensively studied in the field in the past decade. However, less popular materials have recently appeared to respond to the challenges of room-temperature thermoelectrics in terms of sustainability and cost. In this contribution, we comprehensively review the latest advancements in emerging alternative materials with the potential to pave the way for the next generation of sustainable TEGs. This upcoming generation includes flexible and printed TEGs for applications like wearables or the Internet of Things.

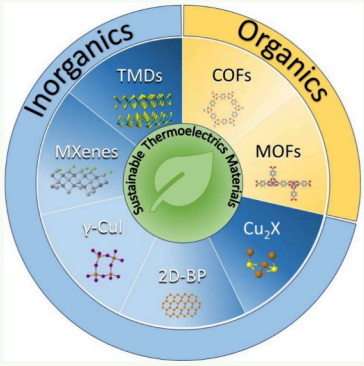

KEYWORDS: *thermoelectric materials, covalent−organic frameworks (COFs), metal−organic frameworks (MOFs), 2D metal carbides (MXenes), transition-metal chalcogenides (TMDs), black phosporus (BP)*

■ INTRODUCTION

In recent years, thermoelectric generators (TEGs) have garnered significant interest as a clean power source owing to their energy-harvesting (EH) capability from waste heat. TEGs offer several advantages over other heat harvesters due to their solid-state nature and reliability.[1]

Owing to these characteristics, TEGs have the potential to be used in various applications, including powering nodes for the Internet of Things (IoT) and waste heat recovery in industries and the automotive sector. Among these applications, energy harvesting is particularly suitable for IoT devices because of the low power consumption of IoT nodes and their distributed nature. IoT nodes currently rely on batteries that have limited lifetimes and environmental concerns related to manufacturing and disposal.[2] Moreover, some of the raw materials required for manufacturing batteries (Li, Co) are scarce and are not readily available in the European Union (EU). In this context, the combination of TEGs with energy storage solutions that can mitigate the blackout moments of TEGs has emerged as an ideal solution for powering the IoT devices.[3−6] In addition to being a power source, TEGs can also be used for fire recognition or temperature sensing.[7−9] Finally, if TEGs can be made flexible, they will become relevant in wearable devices, either as body heat harvesters or as conformable motion and gesture sensors.[10−14]

As illustrated in Figure 1, the principles of thermoelectricity have been well-known since the 19th century, and the first TEGs were developed in the early 20th century. Despite this, their use has been less widespread than other available energy harvesting sources, such as solar cells and electromagnetic devices, likely due to their historical low efficiency (typically between 5 and 10%), especially at low temperatures.

Two thermoelectrical (TE) mechanisms are identified in conducting materials: the Peltier−Seebeck effect and the Thomson effect. The Seebeck and Peltier effects are two sides of a reversible process: the Seebeck effect establishes that when a temperature difference is applied to the junction of two different conductors, an electromotive force is generated between their ends. This process is reversible because a temperature difference appears at the ends of the junctions when current is injected through the junction (Peltier effect). Finally, the Thomson effect describes the heat transfer between a current-carrying conductor subjected to a temperature

Special Issue: Early Career Forum 2024

Received: April 27, 2024
Revised: July 11, 2024
Accepted: July 12, 2024

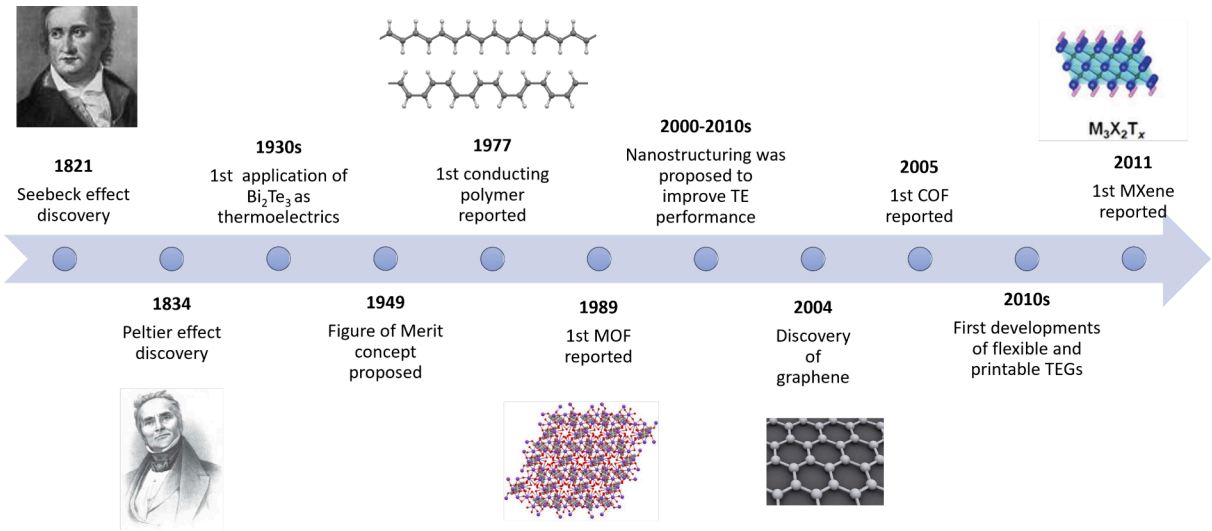

Figure 1. Time line of key developments in thermoelectric technology.

gradient and its environment: heat is emitted if the charge and heat flow in opposite directions and absorbed otherwise. In most practical scenarios, the Thomson effect can be neglected. The performance of TE materials is evaluated through their figure of merit zT, defined as shown in eq 1:

$$zT = \frac{\sigma S^2 T}{\kappa} \tag{1}$$

where σ (S m^{-1}) is the electrical conductivity, S (V K^{-1}) is the Seebeck coefficient, T (K) is the absolute temperature, and κ (W m^{-1} K^{-1}) is the thermal conductivity. The factor $S^2\sigma$ is also known as the power factor (PF). In terms of efficiency, a figure of merit $zT > 1.5$ is considered necessary for a competitive TE material.[15] In this regard, the most competitive thermoelectric materials are inorganic, low-band-gap semiconductors like Bi_2Te_3 or PbTe and their alloys, as they can reach zT values of up to 2 at around 300 K.[16,17] Although these materials have traditionally been rigid and difficult to process over large areas, recent efforts have focused on reducing these obstacles.[18] Organic electronic materials like small molecules and conducting polymers have gained significant attention as viable alternatives to inorganic materials for room-temperature thermoelectric applications. This research is fueled by several advantageous properties, including low material cost, ease of processability via printing techniques, nontoxicity, mechanical flexibility, and low thermal conductivity.[19] (Semi)conducting polymers, such as poly(3,4-ethylenedioxythiophene) (PEDOT), polyaniline (PANi), polypyrrole (PPY), poly(3-hexylthiophene-2,5-diyl) (P3HT), and poly(2,5-bis(3-dodecylthiophen-2-yl)thieno[3,2-*b*]thiophene) (PBTTT), consist of long conjugated molecular chains packed in films with varying degrees of crystallinity, depending on the specific polymer and its deposition process.[20] PEDOT, often blended with poly(4-styrenesulfonate) (PSS), is one of the most studied conducting polymers owing to its good thermoelectric properties and superior ambient stability. The results in the literature show PEDOT-based materials with a figure of merit of approximately 0.46 after using different doping strategies to improve the TE performance.[21−23] Despite being less utilized, PANi, P3HT, and DPP also have applications in performing thermoelectrics.[24] To generate practical TEGs, both p-type and n-type elements are required. However, all of the mentioned polymers are p-type. Developing performing and chemically stable n-type conducting polymers has proven to be a challenge, although recent chemistries have yielded n-type polymers with values of conductivity (>1000 S cm^{-1}) and PF (up to 90 μW m^{-1} K^{-2}) approaching those of their p-type counterparts.[25−27]

In addition to conjugated polymers, carbon-based materials represent another relevant technology involving abundant materials that are compatible with flexible and printed devices. An appropriate combination of polymer and carbon nanomaterials leads to composites with much higher electrical conductivity and PFs than neat polymers. Similar to polymers, n-type composites are difficult to fabricate, and the reported performance is significantly lower than that of the p-type. Most n-type composites are a combination of PEI with a carbon-based nanomaterial and can reach PFs of up to 1500 μW m^{-1} K^{-2} while the highest PF for the p-type composite was as high as 3050 μW m^{-1} K^{-2}. Recently, densified multiwall carbon nanotube (MWCNT) films have led to ultrahigh PF values of 7250 and 4340 μW m^{-1} K^{-2} for p- and n-type materials, respectively. Unfortunately, compared with neat polymers, the increase in the PF of a carbon/polymers composite comes along a large increase in thermal conductivity. As a result, these composites exhibit a moderate, although still better than the zT of polymers, and are not as high as traditional inorganic TE materials.[28]

In recent years, several innovative works have demonstrated other interesting sustainable materials based on nontoxic and nonrare elements for use in thermoelectrics: (i) metal−organic frameworks (MOFs); (ii) covalent−organic frameworks (COFs); (iii) MXenes; (iv) transition-metal dichalcogenides (TMDs); (v) chalcogenides; (vi) black phosphorus.[29] Despite not being able to achieve zT values as high as those of traditionally used materials, most of them are based on abundant/cheap and environmentally friendly elements, some can be printable, and they can operate under mechanical strain, offering a potential future alternative to polymeric and carbon-based thermoelectrics in the development of flexible TEGs. Many reviews have already addressed the TE performance and applications of polymers, carbon-based materials, and their composites.[28,30−32] This review is different because it focuses on emerging sustainable materials that are suitable for near-

https://doi.org/10.1021/acsaelm.4c00770
ACS Appl. Electron. Mater. XXXX, XXX, XXX−XXX

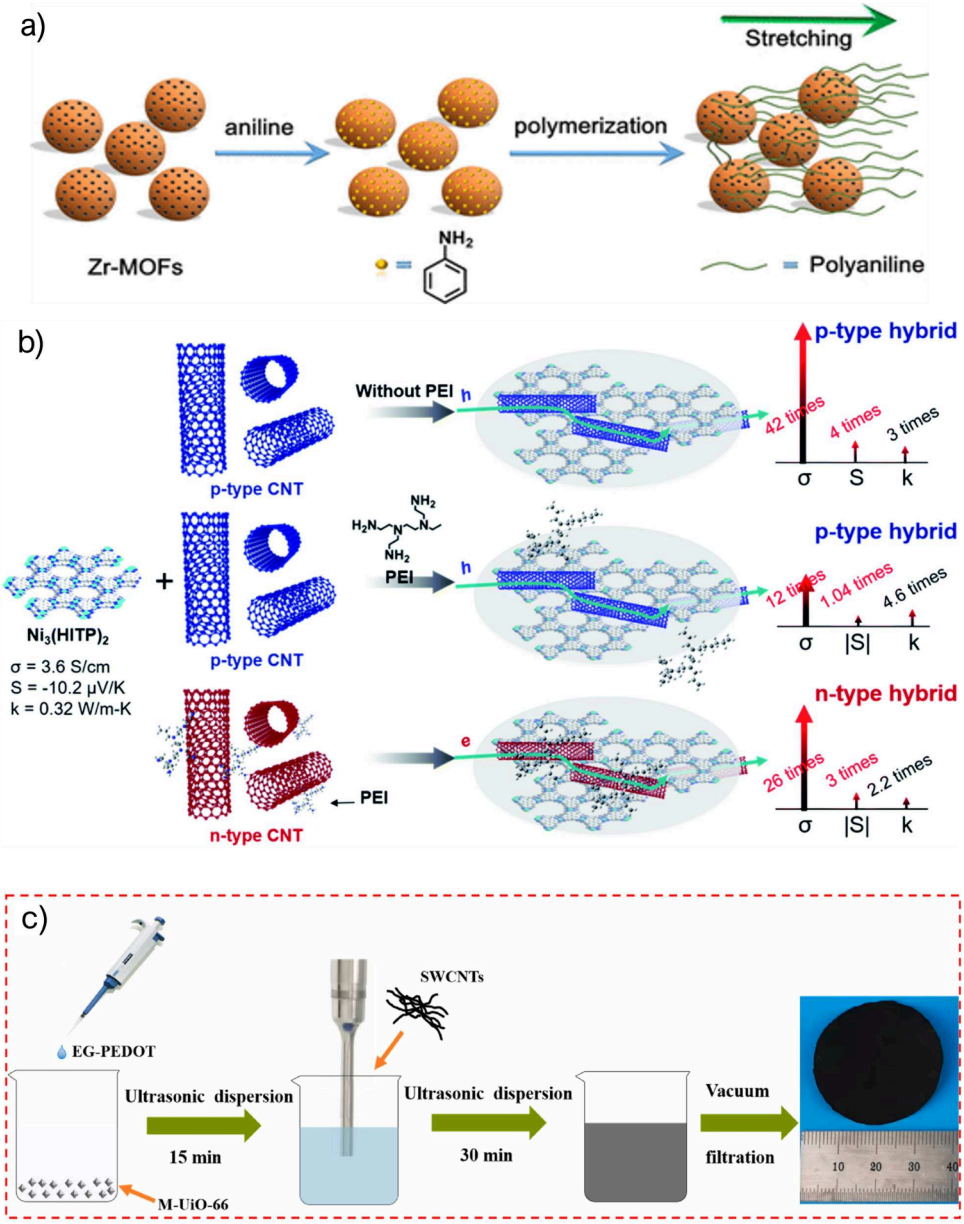

Figure 2. (a) Creation of Zr-MOF/polymer composite. Reprinted with permission from ref 45. Copyright 2018 American Chemical Society. (b) Structure of p- and n-type $Ni_3(HITP)_2$-CNTs hybrids. Reproduced with permission from ref 47. Copyright 2021 Royal Society of Chemistry. (c) Fabrication method of the polymer/SWCNT/MOF hybrid. Reproduced with permission from ref 48. Copyright 2022 Elsevier.

room temperature applications (0−100 °C). In this review, we expect to bring attention to new families of green materials that hold potential in room-temperature energy harvesting for low power applications like the IoT and wearables.

■ FRAMEWORK MATERIALS

Metal−Organic Frameworks (MOFs). MOFs, also known as porous coordination polymers (PCPs), are a new class of tunable hybrid materials resulting from the self-assembly between inorganic units (e.g., atoms, clusters, chains) and organic polycomplexant linkers (e.g., carboxylates, azolates, phosphonates, among other N- and/or O-donor molecules), which have attracted increasing academic and industrial interest.[33,34] Compared with other classical porous materials (e.g., activated carbons, zeolites, and silica), MOFs present high structural and chemical versatility together with very high regular porosity with different shapes and sizes [pore volume up to 4.4 $cm^3\ g^{-1}$; Brunauer−Emmett−Teller surface area (S_{BET}) = 7000 $m^2\ g^{-1}$; pore diameter = 3−98 Å].[35,36] MOFs possess several characteristics similar to those of organic polymers, including nontoxicity and affordability. In contrast to organic conjugated polymers, in which the electronic structure (position of the highest occupied and lowest unoccupied molecular orbitals, HOMO and LUMO levels, respectively) is associated with the delocalized π orbitals of the carbon backbone, in MOFs, the presence of transition metal ions introduces new electronic states from the partially filled d or f orbitals of the metal center, which interact with the organic ligands to form the rich electronic structure of the material.

MOFs offer tremendous synthetic and structural versatility through the selection of metal and organic ligands, which allows the modulation of material electrical and thermal conductivities to optimize zT.[37,38] Furthermore, most notably, their high porosity presents a unique approach to enhancing thermoelectric performance, as the pores effectively scatter phonons, resulting in reduced thermal conductivity and increased zT (eq 1).[39−41] The long-range crystalline order of MOFs plays a crucial role in promoting high charge mobility, thereby increasing the electrical conductivity without significantly

https://doi.org/10.1021/acsaelm.4c00770
ACS Appl. Electron. Mater. XXXX, XXX, XXX−XXX

affecting the Seebeck coefficient. Another distinguishing feature of some MOFs is their exceptional ability to adsorb various molecules and nanostructures within their pores. This property enables fine-tuning or even drastic alteration of the materials' electronic and thermal transport characteristics. The use of MOFs as TE materials is still in its infancy, and only a few conductive MOFs have been explored in TEGs.

In 2020, Park et al. reported the first 3D MOF (Zn-HAB or $[Zn_6C_{24}N_{24}]$, where HAB = hexaaminobenzene; S_{BET} = 145 m^2 g^{-1}) with intrinsic thermoelectric properties. By selecting Zn(II) as a tetrahedral metal node, the authors guided the formation of a 3D structure. Unlike d_9 Cu(II) and d_8 Ni(II) in 2D conductive MOFs, Zn(II) favors a tetrahedral coordination geometry. Its d_{10} configuration results in a 3D MOF with a p-type semiconductive behavior that provides a Seebeck coefficient of 200 μV K^{-1} and a PF of 3.44 nW m^{-1} K^{-2}.[42]

Another interesting MOF is $Cu_3(HHTP)_2$ (HHTP = 2,3,6,7,10,11-hexahydroxytriphenylene). The electrical conductivity of $Cu_3(HHTP)_2$ single crystals was first reported by Hmadeh et al., and it is currently among the best values reported for MOFs (0.2 S cm^{-1}).[43] However, the current challenge is to process MOFs onto solid supports to facilitate their handling. In this regard, Gonzalez-Juarez et al. studied the electrochemical synthesis of $Cu_3(HHTP)_2$ thin films by anodization and their subsequent transfer to poly(methyl methacrylate) (PMMA), addressing the challenge of the lack of substrate. Thinthin film deposition improved the thermoelectric behavior, as the Seebeck coefficient increased accordingly from −7.24 μW K^{-1} for the bulk materials to −121.4 μW K^{-1} for the thin films, and the PF increased from 2×10^{-5} μV m^{-1} K^{-2} to 3.36×10^{-3} μW m^{-1} K^{-2}.[44]

MOFS have also been demonstrated in composites to improve the thermoelectric characteristics of pure organic polymers and carbon nanotubes (CNTs). The first example was the polymerization of aniline in Zr-based MOF UiO-66 or $[Zr_6O_4(OH)_4(BDC)_6]nH_2O$ (H_2BDC = 1,4-benzenedicarboxylic acid), (S_{BET} = 1200 m^2 g^{-1}) using PSS as a dopant.[45] Following the process shown in Figure 2a, the PANi chains interpenetrated into the UiO-66 structure, resulting in a crystalline PANi with improved electrical conductivity. Upon blending with PANI/PSS, the composite exhibits an n-type characteristic, and both the electrical conductivity and the Seebeck coefficient increase with increasing MOF content. Although the thermal conductivity increased slightly with the MOF content, it did so to a lesser extent than the electrical conductivity, resulting in enhanced TE performance. The use of UiO-66 resulted in a Seebeck coefficient of −17.78 mV K^{-1}.

Another elegant MOF-based composite applied in thermoelectrics was reported by Xu et al. In their work, the adsorbed species (free Co^{2+} ions and ligands) found in the pores of a 3D Co-based MOF were exchanged by the conductive ionic liquid 1-ethylpyridinium bromide (EtpyBr) or the photosensitive $AgNO_3$, leading to Co-MOF-Br and Co-MOF-Ag, respectively. The p-type conducting polymer PANi was then introduced into the pores of the MOFs, achieving a maximum Seebeck coefficient of 66.5 μV K^{-1} at 400 K and an electrical conductivity of 0.4 S cm^{-1}. This resulted in a PF of 17 nW m^{-1} K^{-2}. Unfortunately, no value of thermal conductivity was reported.[46]

To further enhance the conductivity of MOFs, they can be combined with CNTs. In particular, Qi et al. hybridized $Ni_3(HITP)_2$ (HITP = 2,3,6,7,10,11-hexaaminotriphenylene) and CNT (30 wt %), leading to a drastic increase in the PF and zT values up to 26 μW m^{-1} K^{-2} and 8.77×10^{-3}, respectively, which is 2 orders of magnitude higher than the zT of pristine $Ni_3(HITP)_2$[47] (Figure 2b). The authors attributed this remarkable improvement to the large increase in both electrical conductivity (from 3.6 to 150 S cm^{-1}, and the p-type Seebeck coefficient (from 10 to 40 μV K^{-1}, induced by the addition of CNTs. When CNTs (typically p-type materials) were doped with polyethylenimine (PEI) to obtain an n-type composite and mixed with the $Ni_3(HITP)_2$, the PF and zT values increased to 9 μW m^{-1} K^{-2} and 3.63×10^{-3} (ca. 70 times), respectively, in comparison with pristine $Ni_3(HITP)_2$. Both n-type and p-type materials were used to develop a TEG with two TE pairs that could generate up to 67 nW for a difference of 60 K. Despite not having a large output power, this example is a landmark in the development of MOF-based TEGs for actual low-power applications. Although the advantages of blending MOFs and CNTs compared with using CNTs alone remain unclear, this work shows that both chemistries are compatible, which opens the door to future synergies.

Flexible thermoelectric composites can be rationally prepared by mixing MOFs and single-walled carbon nanotubes (SWCNTs). Fan et al. presented a flexible thermoelectric material based on a ternary composite built from acetic acid-modified UiO-66 ($[Zr_6O_4(OH)_4]$ clusters with 1,4-benzodicarboxylic acid struts M-UiO-66), SWCNTs, and the conducting polymer PEDOT:PSS treated with ethylene glycol (EG-PEDOT:PSS, Figure 2c). The ternary composite films exhibit good flexibility and enhanced thermoelectric performance compared with EG-PEDOT:PSS. EG-PEDOT:PSS rendered the M-UiO-66 moderately conducting, and the SWCNTs bound all the components as a monolithic flexible film and further boosted the thermoelectric properties, increasing the PF from 0.14 for M-UiO-66/EG-PEDOT:PSS to 27.9 μW m^{-1} K^{-2}, when a 40 wt % of SWCNT is added.[48] Following a similar trend, Chen et al. reported films of SWCNTs@Ni-THT (THT = triphenylenehexathiol). The authors demonstrate how the addition of SWCNTs significantly increases the electrical conductivity of the composite and reduces the Seebeck coefficient at low rates. This effect resulted in a noticeable increase in the PF from 0.001 to 98.1 μW m^{-1} K^{-2} with the addition of 4 wt % SWCNTs. A bending study is detailed, showing a low influence of bending on the thermoelectric properties.[49] Finally, we highlight the work of Xue et al. in the preparation of an SWCNT@MOF flexible composite. Originally, SWCNTs were dispersed in a mixed solution of poly(vinylpyrrolidone) (PVP)/methanol, and $Co(NO_3)_2$ was added to facilitate the Co^{2+} adsorption on SWCNTs surfaces. A mixture of 2-methylimidazole and nano-Co_3O_4 in methanol was slowly titrated into the first suspension, leading to an in situ growth of ZIF-67 ($Co[mim]_2$ [mim = methylimidazole, S_{BET} = 1500 m^2 g^{-1}, pore volume 0.6 cm^3 g^{-1})] on the SWCNT surfaces. Finally, the precomposite was annealed to obtain a flexible and free-standing film (15 μm thickness) of ZIF-67@CNT composite. With the addition of CNTs and the annealing process, the PF increased from 61.6 to 255.6 μW m^{-1} K^{-2}. Furthermore, both the electrical conductivity (825.7 S cm^{-1}) and zT (0.02) at room temperature were the highest in the experimental data reported so far for MOF-related materials, rivaling those reported for polymeric TEs.[50]

As previously mentioned, MOFs share many features with polymer thermoelectrics. However, their distinctive synthetic and structural versatility offers promising opportunities for optimizing electronic structure via a deliberate choice of metals and ligands to achieve both high p-type and n-type zT values. Moreover, such versatility has displayed a tremendous potential for synergy with other materials, such as CNTs and polymers, to deliver composite materials with high TE performance. The capability to generate n-type MOFs in contrast to n-type polymers is noteworthy, especially considering the typical instability of such polymers in the presence of moisture and oxygen.[38,51] Over 90,000 MOFs have been reported to date, and over 500,000 MOF structures have been predicted, providing an unimaginable number of structures to be studied in TEs.[52] Considering the early stage of the application of MOF TEs vs organic polymers,[53] this letter aims to highlight the potential of MOFs in the field of thermoelectrics.

Covalent−Organic Frameworks (COFs). As MOFs, COFs are an exciting new type of crystalline porous polymer that is constructed exclusively with organic building units (no metal ligand involved) via strong covalent bonds. Compared with conventional organic electronic materials, the covalent bond-supported crystallinity of COFs vastly surpasses the intermolecular force-supported crystallinity of semiconducting molecules/polymers, endowing COFs with superior stability. Furthermore, the porous nature of COFs enables mass transport, which is uncommon for traditional conductive or semiconductive materials that are densely packed.[54] These characteristics, along with the flexibility of COFs, make them promising

https://doi.org/10.1021/acsaelm.4c00770
ACS Appl. Electron. Mater. XXXX, XXX, XXX−XXX

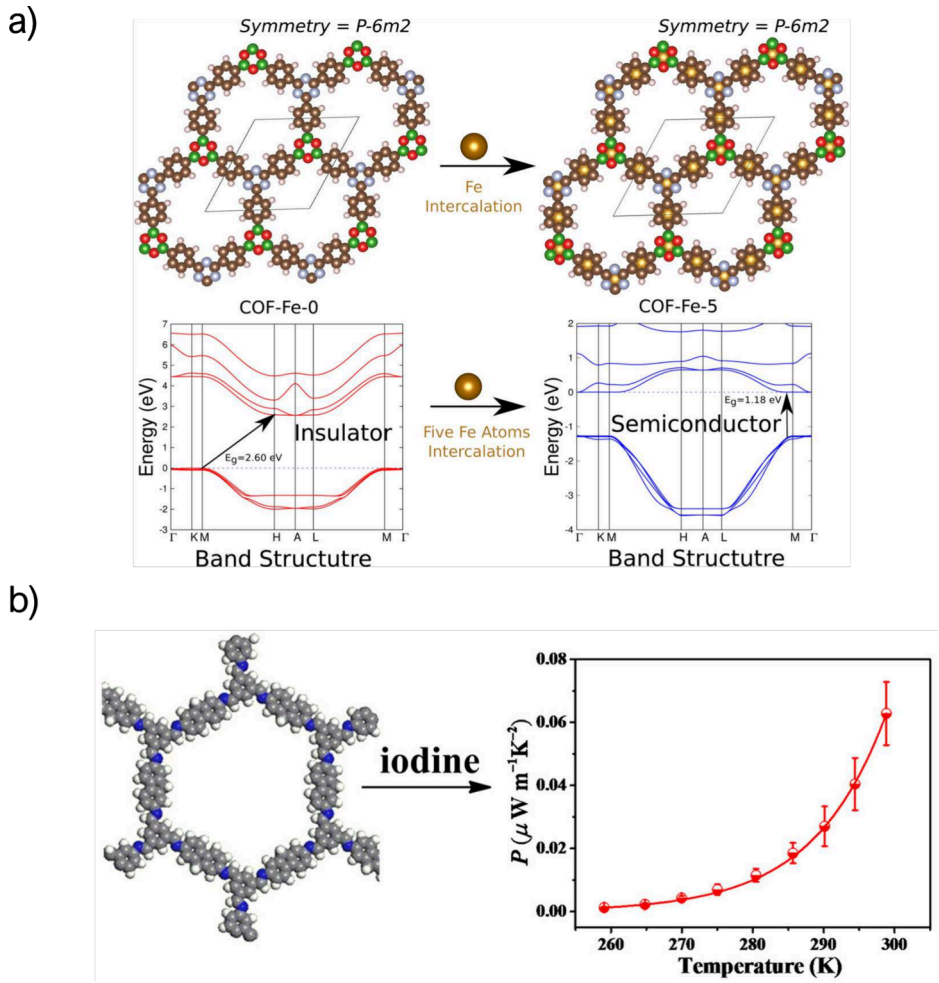

Figure 3. (a) Modification of COF structure with iron ions. Reprinted with permission from ref 57. Copyright 2017 American Chemical Society. (b) Copper/iodine composite structure and thermoelectric performance. Reprinted with permission from ref 58. Copyright 2017 American Chemical Society.

candidates for flexible TEGs. The novelty of COFs in the TE field is appreciated in the reduced number of experimental works in the literature, with only 10 reports on this topic (most of them theoretical).

The first theoretical studies about COF TE properties were focused on their band gap and thermoelectric transport mechanisms, either as raw COF or through modification of the structure. Chumakov et al. reported for the first time calculations based on density functional theory (DFT) and the Boltzmann transport equation to demonstrate the thermoelectric properties of two phthalocyanine (Pc)-based COFs: NiPc and NiPc-benzothiadiazole (BTDA). As expected, due to the organized arrangement of the Pc units and linkers in these COFs, the transport of charge carriers was facilitated by stacking. In all the compounds, the highly directional character of the p orbitals allows band-structure engineering and produces a type of low-dimensional hole transport along the stacking direction of the MOF layers. All compounds investigated are indirect semiconductors. Results show promising characteristics for thermoelectric applications, with a maximum theoretical value of zT around 0.2.[55] More recently, three other COFs based on Pc (Cu-Pc, Zn-Pc, and Co-Pc) were studied by Chumakov and Bayram. The calculations showed even better values than previously reported for Ni-Pc, with zT close to 1 for Cu-Pc and Co-Pc and up to 0.65 for ZnPc.[56] Finally, Pakhira et al. predicted that the electronic properties of COFs can be fine-tuned by adding Fe atoms between two organic layers in the structure. The results presented Fe intercalation as a method to control the band gap of the material and thus the Seebeck coefficient (Figure 3a).[57]

Regarding experimental studies, there are only three experimental works on COF-based thermoelectrics, some of which show promising characteristics. The first study described the condensation of 2,7-diaminofluorene (DAFL) and 1,3,5-triformylbenzene (TFB) to obtain a fluorene-based 2D COF (named FL-COF-1) with high thermal stability and accessible porosity (S_{BET} = 1300 m^2 g^{-1}). The open framework was doped with iodine to improve its electrical conductivity. The compressed pellet of I_2@FL-COF-1 exhibited a Seebeck coefficient of 2450 μV K^{-1} and an electrical conductivity of 1 × 10^{-4} S cm^{-1}, which resulted in a PF of 0.063 μW m^{-1}K^{-2} (Figure 3b).[58] This strategy was also used by Wang et al., in whose work, the I_2 doping of a metal-Pc-based pyrazine-linked 2D COF (named as ZnPc-pz-I_2), led to a notable improvement in the Hall mobility from 5 to 22 cm^2 V^{-1} s^{-1}, making these materials good candidates for thermoelectric applications.[59]

In the third study, the approach followed to prepare n-type COF semiconductors was direct polycondensation of conventional p-type knots with an n-type indigo linker [6,6′-n,n′-(2-methyl)-isoindigovibronic acid or MIDA] to form nonconjugated tetragonal and hexagonal two-dimensional polymeric frameworks. The authors selected knots from a well-known HHTP with a well-established pi-stacking structure, p-type semiconducting behavior, and phthalocyanine (Cu-Pc) as a typical 18-electrons macrocycle with a well-defined planar structure. The resulting HHTP-MIDA-COF and CuPc-MIDA-COF are planar in conformation and show flattened frontier molecular orbital levels, which enable electrons to move along the nonconjugated polymeric backbones. Furthermore, the hall resistance was measured to determine the mobility and carrier type. The authors

https://doi.org/10.1021/acsaelm.4c00770
ACS Appl. Electron. Mater. XXXX, XXX, XXX−XXX

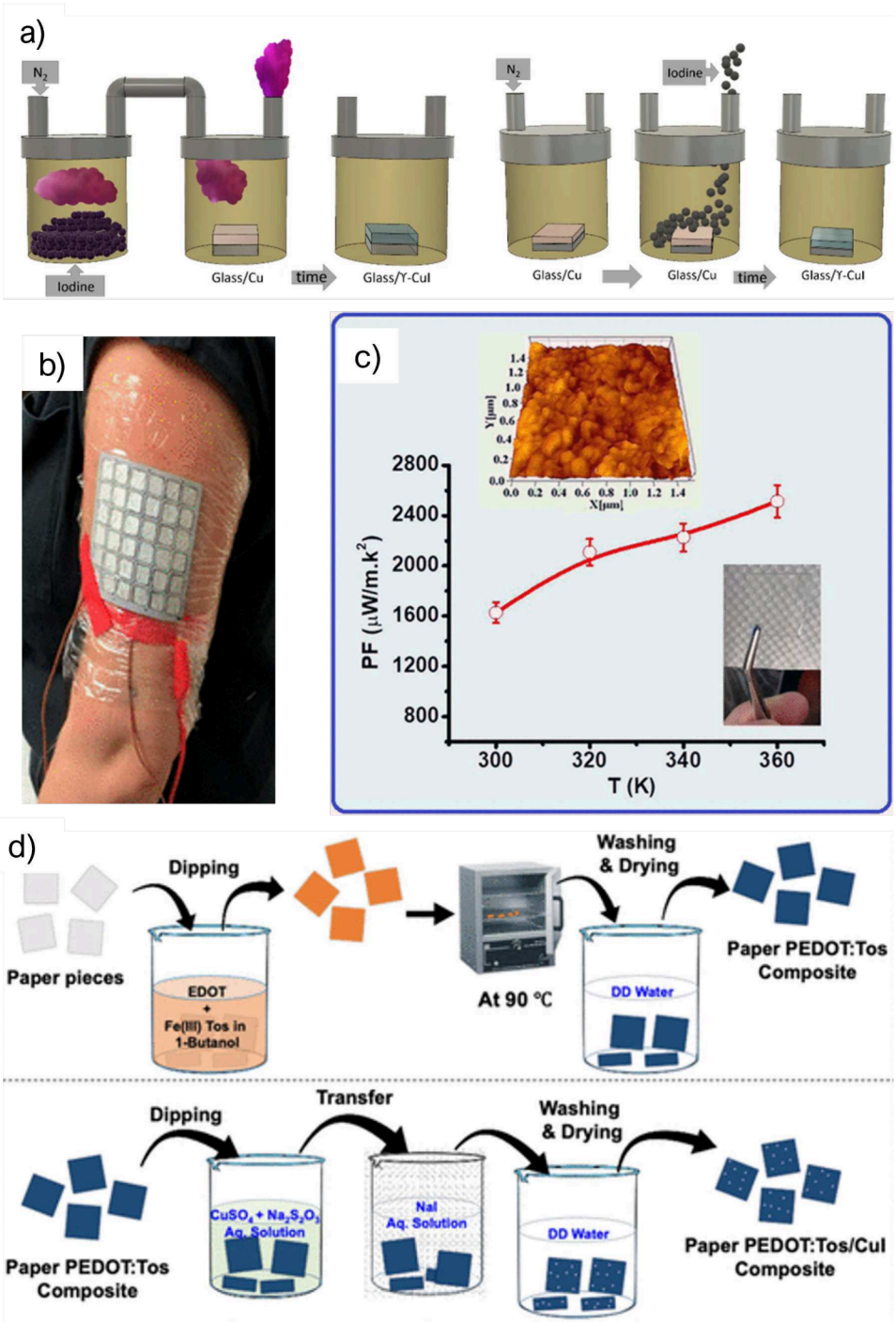

Figure 4. (a) CuI fabrication processes using vapor or solid iodination. Reproduced from ref 72. Available under a CC-BY license. Copyright 2018 Springer Nature. (b) Example of the use of a wearable TEG. Reprinted with permission from ref 75. Copyright 2021 American Chemical Society. (c) PF and details of the CuI TE fabricated by Almasoudi et al. Reprinted with permission from ref 73. Copyright 2022 American Chemical Society. (d) Process used to prepare the PEDOT:Tos/CuI composite. Reprinted with permission from ref 75. Copyright 2021 American Chemical Society.

obtained a high electron mobility of 8.2 $cm^2 V^{-1} s^{-1}$, which makes these materials promising candidates for n-type thermoelectrics.[60]

Similar to MOFs, COFs have very versatile structures that allow them to tune their thermoelectric characteristics. However, their application in the TE field has been barely studied in the literature; thus, there is still a long way to make them competitive in terms of TE performance.

Metallic Chalcogenides. In addition to well-known group V−VI chalcogenides, metal chalcogenides like Ag chalcogenides and Cu chalcogenides have emerged as promising TE materials. In particular, the latter compounds have attracted intensive interest recently. They have the formulation Cu_2X, where X denotes Se or S. These compounds are p-type semiconductors that exhibit exceptional electrical and thermal transport characteristics and thus have a high figure of merit at medium to high temperatures. The compounds with Se showed better performance and were more studied in the literature than those with S. S compounds are more suitable for this review because S is less toxic and more abundant than Se. This lack of

https://doi.org/10.1021/acsaelm.4c00770
ACS Appl. Electron. Mater. XXXX, XXX, XXX−XXX

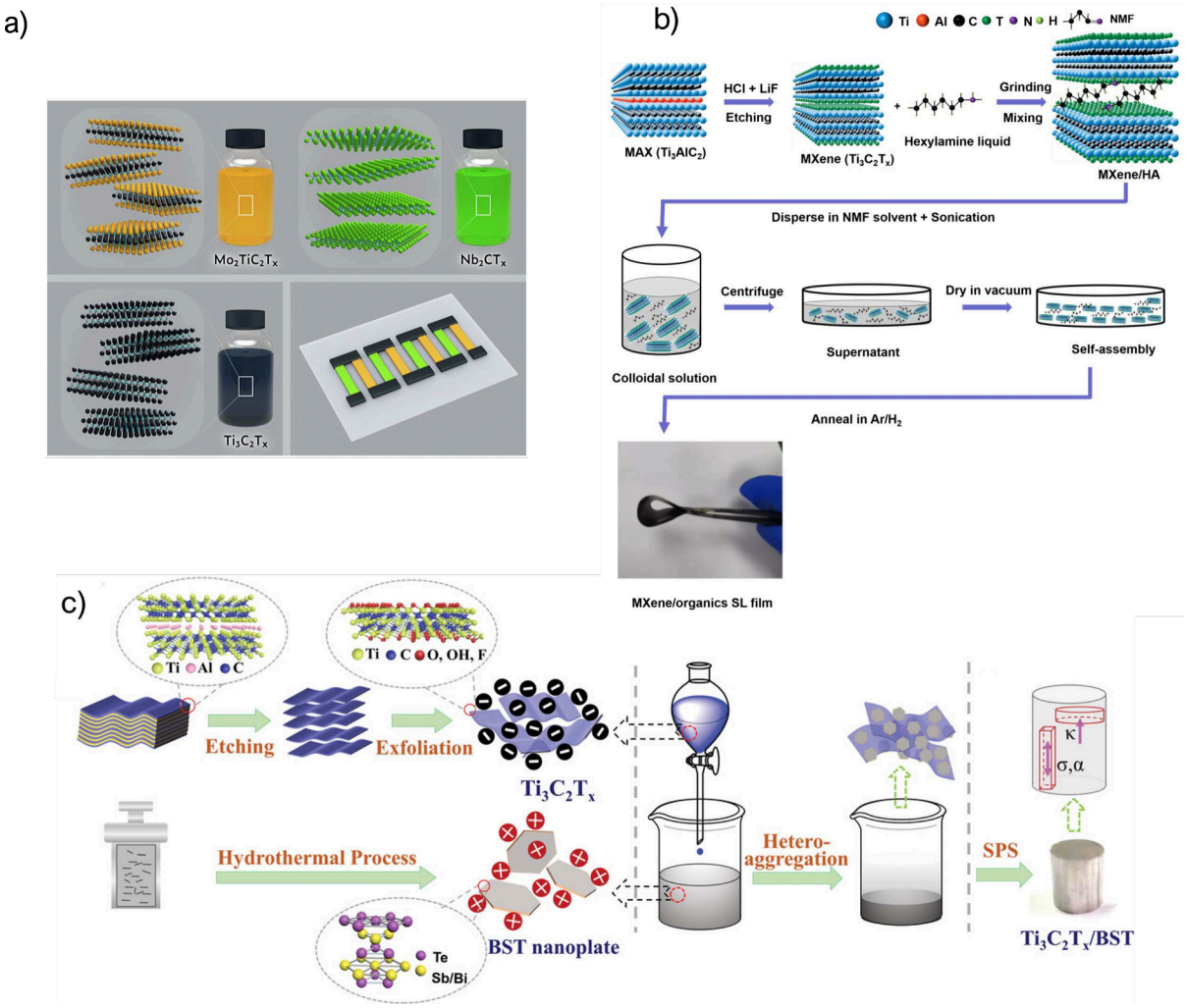

Figure 5. (a) All MXenes used in the TEG fabrication. Reprinted with permission from ref 80. Copyright 2022 Elsevier. (b) Fabrication method of MXene and an organic superlattice flexible thermoelectric compound. Reprinted with permission from ref 82. Copyright 2022 American Chemical Society. (c) Fabrication methods of BST and MXene thermoelectric materials. Reprinted with permission from ref 87. Copyright 2019 Wiley.

toxicity contrasts with the IV−VI and V−VI chalcogenides, which contain Pb and Sb.[61−64] Furthermore, Cu is less scarce and cheaper than Pb, Sb, or (especially) Bi, which are typically used in IV−VI and V−VI TE.[65]

Recent works on Cu_2S shows that it can reach high zT and PFs at high temperatures. The first attempt to print Cu_2S was in 2019 by Burton et al., who fabricated a 3D-printed TE with a zT of 0.63 at 966 K. This is a low value compared with other studies on bulk Cu_2S,[67] but the study presents the advantage of a printable and scalable method for TE materials.[66] More recently, Yue et al. achieved a zT close to the highest value reported for Cu_2S[67] using a simple fabrication method. They developed a hydrothermal process to develop a micro/nano $Cu_{2-x}S$ composite which thanks to its low thermal conductivity (0.69 W m^{-1} K^{-1}), it reached a zT value of 1.1 at 773 K. These results demonstrate that Cu_2S compounds are perfect candidates to fabricate TE devices with good performance.

Further improvement of the performance of Cu_2S can be possible using dopants, as studied by Zhang et al. In this work, the authors tested several dopants, including In, Cd, Zn, Sn, and Pb. The doped composites were fabricated using a colloidal solution of nanoparticles that, once doped, were dried and annealed at 400 °C; finally, the composites were hot-pressed to form pellets. From the results obtained, we concluded that Pb is the most interesting dopant from a performance perspective because the Pb-doped Cu_2S pushes the zT to 2.03 at 900 K. This is the highest zT reported for Cu_2S. These outstanding results are attributable to the need to use toxic Pb.[69] Although the temperature at which these impressive results are achieved limits the application of these sustainable and abundant materials to specific scenarios, such as the automotive industry[68] future developments might increase their performance may increase at lower temperatures relevant for pervasive electronics. This prospect makes it worthwhile to closely monitor progress in the field over the next years. Other authors have tried to exploit the use of Cu_2S at low temperatures by blending it with polymers.; it is the case of Zhao et al., who studied the influence of Cu_2S in PEDOT:PSS screen-printed TE films. The composite was characterized at content ratios of 1:1.1 to 1:1.4 of Cu_2S and PEDOT:PSS, respectively. The results show that the conductivity increases with increasing PEDOT:PSS content, whereas the Seebeck effect is reduced. Consequently, the change in PF is not significant among the different concentrations; the highest PF is 20 μW m^{-1} K^{-2} for a 1.2 ratio, while the lowest was 18 μW m^{-1} K^{-2} for a 1.1 ratio. The authors demonstrated the utility of this material by creating a TEG using Ag_2Se for the n-type legs. This device was able to generate up to 160 nW for a temperature difference of 35 K, which in comparison to other Cu_2S results is not very high, but probably because the top performance of Cu_2S was obtained at nonpractical high temperatures (around 900 K).[70]

γ-CuI. γ-CuI is a transparent p-type semiconductor that has been extensively used as a transparent electrode in solar cells, displays, and light-emitting devices. The applications of γ-CuI in thermoelectric fields have been studied. This material is interesting because it is

https://doi.org/10.1021/acsaelm.4c00770
ACS Appl. Electron. Mater. XXXX, XXX, XXX−XXX

nontoxic. γ-CuI has a wide band gap (3.1 eV) and reduced thermal conductivity because iodine is a heavy element.

Yang et al. studied the influence of carrier concentration on thin films of γ-CuI fabricated via reactive sputtering. Their results showed a maximum zT of 0.21, a carrier concentration of 10^{20} cm^{-3}, and a PF of 375 μW m^{-1} K^{-2} at 320 K. Furthermore, they studied their behavior as a one-leg TEG, achieving an output power of 8 nW at a difference of temperature of 10K.[71] More recently, Morais Faustino et al. presented three fabrication methods for CuI: thermal evaporation of CuI powder, vapor iodination of Cu films, and vapor iodination. The best result was achieved for solid iodination and corresponded to a PF of 470 μW m^{-1} K^{-2}. Finally, they developed a TEG using gallium-doped zinc oxide (GZO) as the n-type leg. With this structure, the authors achieved an output power of 0.45 nW at a temperature difference of 13 K. This value of output power is lower than expected for a high PF measured. In 2022, Almasoudi et al. used the pulsed laser deposition to iodinate Cu. With this method, they achieved an outstanding PF of 2400 μW m^{-1} K^{-2} and a zT of 1.12 at 360 K, as shown in Figure 4c. Furthermore, the resulting film is flexible and transparent, making it a perfect candidate for wearable applications[73]

Other authors like Salah et al. and Maji et al. studied the possibility of using other elements to improve the performance of CuI. First, Salah et al. studied several possible dopants, including metals, semimetals, and rare earths. The best result was obtained by doping CuI nanoparticles with 0.05 mol % Tb, which increased the zT from 0.05 for pristine CuI to 0.28 at 420 K.[74] Another innovative strategy followed by Maji et al. was to fabricate a composite of PEDOT:Tos and CuI on a paper substrate following the process illustrated in Figure 4d. Compared with neat PEDOT:Tos, the addition of CuI increased the Seebeck coefficient from 63 to 225 μV K^{-1}. Finally, the authors developed a device composed of 36 legs of this TE connected in series (Figure 4b) that could produce up to 57.9 nW from human body heat (a temperature difference of around 4 K).[75]

■ 2D INORGANIC MATERIALS

MXenes. MXenes are layered transition-metal carbides, carbonitrides, or nitrides discovered in 2011.[76] MXenes are obtained from layered ternary materials known as $M_{n+1}AX_n$ or MAX phases, which are a large group of layered hexagonal compounds, where M is a transition metal, A is an A-group element (mostly groups 13 and 14), X is C or N, and n is 1−3. When the A-layers are chemically etched, the result is weakly bound stacks of 2D sheets with a $M_{n+1}X_nT_x$ composition, where T_x represents the surface termination.[77] These materials are 2D materials with promising applications, most of them in the energy field as storage elements, electromagnetic shielding, and, more recently, also as TE.[78] MXenes have the advantage of being nontoxic, abundant materials in contrast to traditional inorganic materials like group V−VI chalcogenides. Moreover, recent progress in process scalability and shelf life has suggested their viability for industrial applications.[79]

Very recently, MXenes based on $Mo_2TiC_2T_x$ or Nb_2CT_x have been used for thermoelectricity with high PF, as demonstrated by Huang et al.[80] The authors developed a full MXene TEG (Figure 5a), where the n-type leg was made of $Mo_2TiC_2T_x$, the p-type leg of Nb_2CT_x, and $Ti_3C_2T_x$ was used for contacts. TEG was fabricated using a combination of screen printing, poly(dimethylsiloxane) (PDMS) masking, and dropcasting. With these materials, the authors reached a PF of 13.26 μW m^{-1} K^{-2} for the n-type MXene and 11.06 μW m^{-1} K^{-2} for the p-type. The final device can provide up to 35 nW for a temperature difference of 30 K using 20 TE pairs, which is a low value compared with other works; for example, Qi et al. achieved 65 nW using only two pairs. However, the work of Huang et al. is remarkable due to the achievement of an n-type TE material, which is more challenging to obtain than a p-type.

The TE performance of pure MXenes can be enhanced in several ways. Liu et al. demonstrated that through strong basic treatment (KOH under hydrothermal conditions), the TE behavior of $Ti_3C_2T_x$ can be improved. Through this process, some F-terminal groups of the MXenes were replaced by K, increasing the electronic band gap of the material. This resulted in a significant improvement in the Seebeck coefficient from 6.6 to 44.98 μW m^{-1} K^{-2}. On the other hand, the electrical conductivity is reduced as the KOH content in the reaction increases. An optimal point at which the PF was maximized to 45 μW m^{-1} K^{-2} is found when the KOH concentration was 12 mmol. Unfortunately, the authors did not provide any information on thermal conductivity, making it impossible to determine the figure of merit. Nonetheless, a flexibility study was presented, reporting variations in the PF of less than 10% after 1000 bending cycles.[81] Following a different strategy, Wang et al. enhanced the carrier mobility and density of a $Ti_3C_2T_x$-organic superlattice using the process shown in Figure 5b.[83] In this work, MXene was combined with hexylamine (HA), resulting in a flexible film with n-type thermoelectric behavior. When annealed at 150 °C, the composite exhibited a PF of 33 μW m^{-1} K^{-2}.

Sarikurt et al. investigated the thermoelectric properties of oxygen-functionalized MXenes. A theoretical analysis was employed to examine the thermal transport and thermoelectric characteristics of various MXenes, specifically those with the composition M_2CO_2 (where M = Ti, Zr, Hf, Sc), considering two distinct crystalline structures. The relaxation time approximation was used to predict the thermoelectric parameters of MXenes under both n-type and p-type doping conditions. The results revealed a notable theoretical zT value of 1 at moderate carrier densities across all examined crystalline structures, with particularly high Seebeck coefficients observed for Zr_2CO_2 and Hf_2CO_2. This suggests that oxygen-functionalized MXenes exhibit promising potential as thermoelectric materials.[84]

Following a similar trend to that of MOFs, the use of MXenes in the thermoelectric field has led to the preparation of composite materials to improve their thermoelectric performance. Chalcogenides and other inorganic compounds (i.e., ZnO) are common materials used in the preparation of MXene composites for TEG because their characteristics can be improved using MXenes. One example is the study of Guo et al., in which an improvement of 78% in zT is achieved when adding Mo_2CT_x to Bi_2Te_3.[85] Other reports use $Ti_3C_2T_x$ and bismuth antimony telluride (BST) compounds, leading to an improvement of up to 48% in zT (Figure 5c).[86,87] More examples of enhanced thermoelectric properties are the composites based on the chalcogenides GeTe, SnSe, and SnTe with $Ti_3C_2T_x$ achieving exceptional PF values up to 2000 μW m^{-1} K^{-2}.[88−90] Although these chalcogenides include rare and/or toxic elements, which are not covered in this review, these examples are still interesting because they illustrate the potential of mixing MXenes with benchmark materials.

Indeed, the thermoelectric performance of more sustainable inorganic compounds other than chalcogenides can be further improved using MXenes. The work by Yan et al. demonstrated the strategy of depositing ZnO layers on $Ti_3C_2T_x$ films by atomic layer deposition (ALD). With this method two effects was observed: the Seebeck effect was magnified by the increased mobility of high-energy carriers, and the thermal conductivity was reduced. Thus, the overall zT was highly enhanced, reaching a value of 1.8×10^{-3} at 625 K, which, despite being a low value, was four times higher than that of pristine MXene films.[91] In a similar study, the thermoelectric characteristics of Cu iodide were enhanced by blending it with $Ti_3C_2T_x$ in a composite. The results show that a boost in carrier density coming from $Ti_3C_2T_x$ produced an electrical conductivity improvement. Only 5 vol % of MXenes improved the figure of merit 5 folds compared to pristine CuI, and led to a PF value as high as 100 μW m^{-1} K^{-2} at 400 K.[92]

Other less studied materials used in the preparation of MXene-based TE composites include single-wall carbon nanotubes (SWCNTs), organic polymers, and perovskites. One interesting work was reported by Wei et al. on the preparation of a p-type structure composed of SWCNTs and $Ti_3C_2T_x$. The best performance was achieved with 10 wt % of MXene. SWCNT@$Ti_3C_2T_x$ reached a PF value of 203.23 μW m^{-1} K^{-2} at room temperature, and a zT 20-fold higher than pristine SWCNT.[93] Another example of SWCNT@MXene composite was presented by Ding et al. This time, the prepared composite was a sandwich structure of $Ti_3C_2T_x$/SWCNT/

https://doi.org/10.1021/acsaelm.4c00770
ACS Appl. Electron. Mater. XXXX, XXX, XXX−XXX

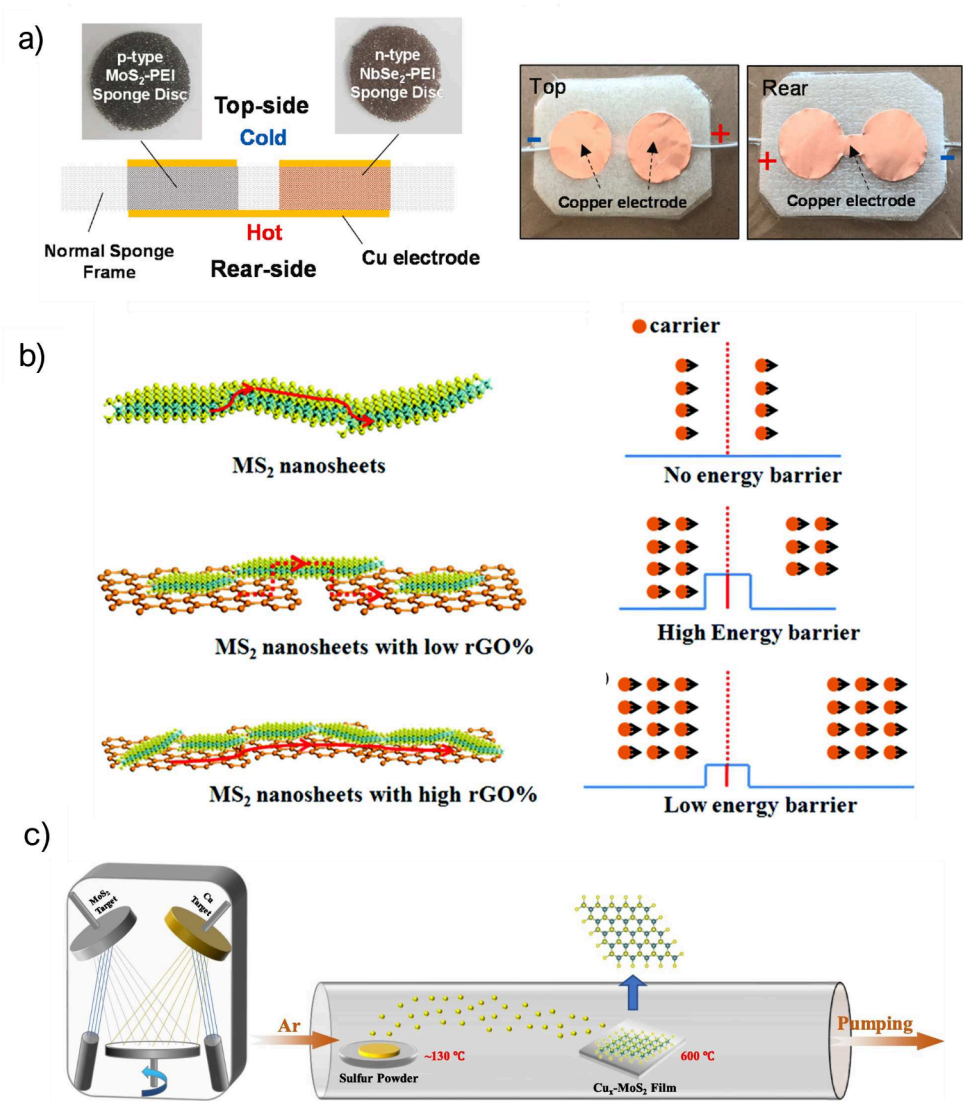

Figure 6. (a) Deformable TEG based on n- and p-type TMDs. Reprinted with permission from ref 107. Copyright 2023 Elsevier. (b) Filtering effect of adding rGO to MS_2. Reprinted with permission from ref 113. Copyright 2017 Royal Society of Chemistry. (c) Fabrication process of Cu-MoS_2 hybrid films. Reprinted with permission from ref 115. Copyright 2023 Elsevier.

$Ti_3C_2T_x$, which enhanced the electrical conductivity of the material, and thus, the PF, which was increased by 25-fold (from 3.12 to 77.9 μW m^{-1} K^{-2}) compared with that obtained with neat $Ti_3C_2T_x$.[94] In the use of organic polymers in the preparation of MXene-based composites, it should be noted the work of Guan et al. In this work, the $Ti_3C_2T_x$ was included in the structure of PEDOT:PSS, generating an energy-filtering effect that increased the Seebeck coefficient of the compound. This filtering effect was observed only at MXene concentrations under 33 wt %, as this ensured that the MXene sheets were not connected between them. Through this mechanism, the authors reported an increase in the Seebeck coefficient from 23 to 57.3 μV K^{-1} while the electrical conductivity was reduced from 800 to 150 S cm^{-1}, thus increasing the PF from 40 to 155 μW m^{-1} K^{-2}.[95] Finally, $Ti_3C_2T_x$ MXenes also improved the n-type oxide perovskite $SrTi_{0.85}Nb_{0.15}O_3$ (STN) thermoelectric properties. Thanks to the inclusion of MXenes in the STN, electron mobility was enhanced, and the conductivity of the compound was significantly increased. As a result, the authors of this work achieved an outstanding increase of zT of 7-fold, which reached a value of 0.9 at 900 K and a PF of 3000 μW m^{-1} K^{-2} at 500 K. Furthermore, the authors presented a device prototype with four legs of STN + 1 wt % MXene that can generate up to 38 mW at a temperature difference of 713 K. This power output could be sufficient to power a sensor node without a battery or with the backup of a supercapacitor.[96] However, these impressive values were achieved at very high temperatures, which limits the applicability of this material in the field of pervasive electronics.

Transition-Metal Dichalcogenides (TMDs). TMDs are 2D materials with a formulation of MX_2 based on a chalcogenide (X) and at least one electropositive element (M). These materials have garnered a lot of interest in recent years due to their interesting electrical properties, including thermoelectricity.[97] TMDs show a high PF due to their high Seebeck coefficient and high electrical conductivity; however, their figure of merit is limited by their high thermal conductivity.[98]

One of the most promising TMDs for thermoelectricity is theoretical materials based on Mo and W.[99] Several theoretical works have reported on their TE properties,[100−103] such as the work developed by Ouyang et al., providing the calculated highest performance of $MoS_2/MoSe_2$ hybrids nanoribbons with a figure of merit of 7.4 at 800 K; or the first-principles calculations carried out by Purwitasari et al., where Tc-based TMDs can reach a figure of merit of 1.8 at 1200 K.[104]

On the other hand, there are a few experimental works on thermoelectrics that are based exclusively on TMDs and are based on toxic materials like Se or Te.[105,106] Nghia et al. showed a TEG based on p-type MoS_2 and n-type $NbSe_2$. In this work, the authors used

https://doi.org/10.1021/acsaelm.4c00770
ACS Appl. Electron. Mater. XXXX, XXX, XXX−XXX

poly(ether imide) (PEi) and a melamine sponge as substrates to fabricate a flexible device to be adhered to the skin, obtaining energy from body heat. The device is shown in Figure 6a. The results show a figure of merit of 5.4×10^{-3} and a PF of 0.537 μW m^{-1} K^{-2} for the p-type material and a figure of merit of 1.36×10^{-3} and a PF of 0.035 μW m^{-1} K^{-2} for the n-type material. Although the results obtained were not exceptionally high, their application closely aligns with wearable TEG.[107] All of these studies present results that are clearly worse than theoretical studies, which means that there is still plenty of room for improvement.

A recently studied n-type material is TiS_2 monolayers. While layered TiS_2 bulk was already known, and the intercalation of transition metals on TiS_2 with very high performance (PF = 37.1 μW m^{-1} K^{-2} and zT = 0.16 at 300 K) was reported in 2011, it was not until 2011 that monolayers were suggested as a promising material for thermoelectricity at low temperature.[108,109] More recently, Li et al. demonstrated by first-principles calculations that the performance of TiS_2 can be enhanced by applying strain to the material. This point was experimentally confirmed by Salah et al., who were able to fabricate TiS_2 pellets with high TE performance at room temperature. In the same study, the authors demonstrated that the strain generated by contraction at low temperatures increased the output power of a single leg by six times and achieved a PF of 540 μW m^{-1} K^{-2}. Despite these exciting results, the authors reported only a modest value of zT = 0.04 at temperatures above RT (up to 100 °C).[110,111] Another strategy that has demonstrated good results in enhancing the performance of neat TiS_2 is microstructural texture engineering. Gu et al. realized an ethanol-based pulverization process followed by Spark Plasma Sintering to produce highly textured and small-grain ceramics. Compared with the pristine synthesized powder, the enhanced PF was driven by the high texture and reduced thermal conductivity resulting from the small grain size. These improvements resulted in an increase of 75% in zT (from 0.4 to 0.7) and 65% in PF (from 1 to 1.7 mW m^{-1} K^{-2}).[112]

Similar to the other materials reviewed in this study, TMDs can also be used to fabricate TEG composites. The composites discussed in the literature, as anticipated from theoretical studies, predominantly involve MoX_2 TMDs. For instance, Wang et al. investigated the impact of reduced graphene oxide (rGO) on the thermoelectric properties of MoS_2 and WS_2. This hybrid material exploits the junction effect between rGO and TMDs, creating an energy barrier that filters low-energy carriers, as represented in Figure 6b. This resulted in an enhancement of the Seebeck coefficient. Remarkably, the electrical conductivity also increased, which consequently improved the PF. The authors achieved a PF of 15.1 μW m^{-1} K^{-2} for the MoS_2 composite and 17.4 μW m^{-1} K^{-2} for the WS_2 composite, marking a 1.5 times improvement compared to pristine TMDs. These results resulted in zT values of 0.022 for MoS_2 and 0.025 for WS_2.[113]

Furthermore, several examples exist in which metallic particles have been employed to enhance the thermoelectric performance of pristine TMDs. For example, the thermoelectric performance of MoS_2 can be further improved through decoration with Ag nanoparticles, as demonstrated by Li et al.[114] The Ag@MoS_2 composite presented in this work attained a PF of 30.3 μW m^{-1} K^{-2}. Cu is another candidate for doping MoS_2, as demonstrated by Xin et al. In this study, MoS_2 was doped with Cu by magnetron sputtering followed by chemical vapor deposition (CVD) (Figure 6c). Finally, the compound was annealed at 600 °C. The PF of this composite was 1.25 μW cm^{-1} K^{-2}, and the figure of merit was 0.137 at 450 K, which improved the zT by an order of magnitude compared to pristine MoS_2.[115] More recently, Yang et al. achieved outstanding thermoelectric performance in MoS_2 by adding aluminum. The Al@MoS_2 compound exhibited a PF of 122 μW m^{-1} K^{-2}, nearly double that of neat MoS_2.[116]

TiS_2 have been also extensively used along with organic polymers. For example, Wan et al. manufactured an n-type thermoelectric by intercalating phenylammonium between layers of TiS_2. With this structure, the new materials maintained the PF while reducing 7 times the thermal conductivity, which resulted in a zT of 0.28 at 370 K (3 times higher than a single TiS_2 crystal).[117−119] Another strategy presented by Wang et al. was the combination of TiS_2 with fullerene. In this study, we developed a method to intercall fullerene between TiS_2 layers. The composition of the hybrid films was optimized to maximize the thermoelectric performance at a 1 wt % of C_{60}. At this composition, the hybrid films achieved an outstanding zT of 0.3 and a PF of 375 μW m^{-1} K^{-2} at 400 K. Furthermore, we fabricated a TEG with PEDOT:PSS as the p-type legs. This device can generate up to 350 nW at a temperature difference of 20 K with only two pairs of TE legs. These works present TiS_2 as one of the best TMDs for flexible, nontoxic, and room-temperature thermoelectric materials because it exhibits an experimental zT higher than those of the TMDs.[120]

Finally, TaS_2 with covalently bonded organic groups was investigated by Wang et al.[121] This process improved the zT of the material by 10-fold compared to neat TaS_2, reaching a PF of 340 μW m^{-1} K^{-2}, which is the best-reported result for TMD composites. However, the high thermal conductivity limited the zT to 0.04. As reviewed, the TMD family has experienced steep progress over the last year, especially regarding PF, and these materials hold great potential for sustainable and performing room-temperature TEs.

Black Phosphorus. Black phosphorus has been known in bulk since 1914; however, it has recently reemerged as a 2D material owing to its layered structure.[122] 2D black phosphorus is a p-type monatomic 2D semiconductor composed of atomic layers stacked by van der Waals forces. This structure allows the generation of few-layer and monolayer BPs via liquid-phase exfoliation (LPE). Exfoliation of the BP enables modification of the band gap, which increases with decreasing number of layers. The thermoelectric properties of BP have been recently explored, making it a candidate for nontoxic flexible TE materials.[123]

2D BPs are truly novel materials, and most of the recent literature on the thermoelectricity of 2D BPs consists of theoretical works.[124,125] Theoretical studies have predicted a Seebeck coefficient of over 300 μV K^{-1} and a zT of up to 1.2 at 500 K.[125,126] Furthermore, the TE properties are highly anisotropic in layered BP, being higher in the armchair direction as the thermal conductivity is noticeably lower. More recently, Zeng et al. reported a study on the TE properties of BP, experimentally demonstrating its anisotropic properties of the material. They obtained a zT of 0.043 in the armchair direction, whereas the zT in the zigzag direction was 5.5 lower, i.e. 0.0075.[127]

At the experimental level, the greatest challenge in BP is to achieve stable monolayers; however, some recent reports have demonstrated the synthesis of monolayers.[128] For example, Novak et al. obtained BP flakes via ball milling and red-phosphorus filtering. After this processing, the BP was mixed with PEDOT:PSS to improve its TE performance. The composite reached the highest PF when a 2 wt % of BP was mixed with PEDOT:PSS with a value of 36.2 μW m^{-1} K^{-2}, representing an increment of 2.09 times that of neat PEDOT:PSS.[129]

■ CONCLUSIONS

In this work, recent advances in green TE materials for near-room-temperature applications and examples of such materials in flexible and printed devices are reviewed. In particular, we focused on MOFs, COFs, MXenes, CuI, TMDs, black phosphorus, and their composites. The first two materials are organic or hybrid, whereas the others are pure inorganic. Table 1 shows a compilation of the literature reviewed in this study.

Organic and hybrid materials are excellent options for flexible TEGs; however, their performance is lower than that of inorganic materials. Despite these disadvantages, all the works reviewed in the field of organic materials used nontoxic elements and were flexible. From the organic materials reported, the most promising are COF, as theoretical studies predict figures of merit close to 1, although the performance shown in experimental works is still low.

Within inorganic materials, MXenes are a great choice for composites to fabricate flexible and printable TEGs. However, the performance of the neat materials was low. Advances in the inorganic realm are more significant for metallic chalcogenides.

https://doi.org/10.1021/acsaelm.4c00770
ACS Appl. Electron. Mater. XXXX, XXX, XXX−XXX

Table 1. Comparative between Different Works Reviewed in This Publication

material	PF (μW m^{-1} K^{-2})	zT	ref
Zn-HAB	0.344		42
Zr-MOF + PANi	664		45
$Ni_3(HITP)_2$ + CNT	24.86	0.0012	47
Ni-THT + SWCNTs	98.1		49
M-UiO-66 + PEDOT + SWCNT	27.9		48
MOF/SWCNT		0.02	50
F-COF + iodine	0.063		58
$Mo_2TiC_2T_x/Nb_2CT_x$	13.26/11.06		80
$Ti_3C_2T_x$ + KOH	44.98		81
Ti_3CAlC_2 + hexamine	33		82
Bi_2Te_3 + Mo_2C	570	0.25	85
$Ti_3C_2T_x$ + SnTe	2000		90
MXene + GeTe	40	1.12	88
$Ti_3C_2T_x$ + SnSe		0.93	89
$Bi_2Te_{2,7}Se_{0,3}$ + $Ti_3C_2T_x$	1.49×10^3	0.68	86
$Ti_3C_2T_x$ + BST		1.3	87
$SrTi_{0,85}Nb_{0,15}O_3$	3000	0.9	96
$MoS_2/NbSe_2$	0.537/0.035	$5.4 \times 10^{-3}/1.36 \times 10^{-3}$	107
TiS_2	540	0.04	111
TiS_2	1700	0.7	112
WS_2 + rGO	17.4		113
MoS_2 + Ag	30.3		114
MoS_2 + Cu	125		115
MoS_2 + Al	122		116
TaS_2	340	0.04	121
TiS_2 + hexylammonium		0.28	117
TiS_2 + fullerene	375	0.3	120
Cu_2S	10.1	1.1	68
Cu_2S + Pb		2.03	69
Cu_2S + PEDOT:PSS	20.3		70
BP + PEDOT:PSS	36.2		129
CuI	375	0.21	71
CuI	470		72
CuI	2400	1.12	73
CuI + Tb		0.28	74

These materials reach a zT of around 1.1, which is very close to the milestone of 1.5 suggested for being competitive with other renewable energy sources,[15] despite this zT is reached a higher temperature than the maximum zT for organic materials. It is remarkable that many works in this family presented better TE performance than other inorganic materials, but they rely on the use of toxic Se, which makes them unsuitable for green applications. The best result found in the literature is Pb-doped Cu_2S, that reaches a figure of merit of up to 2.03. However, the use of Pb at low concentrations renders this compound far from green..

TMDs and BPs are barely studied materials, but theoretical studies show promising TE performance (zT up to 1.8 for TMDs). However, their experimental performance is still far from those predictions, which suggests that these materials still have significant potential for improvement and represent a major opportunity for the field of TEs. The potential of TMDs was already partially fulfilled by TiS_2, which stood out with an impressive experimental zT = 0.7 around room temperature.

Finally, γ-CuI has recently emerged as a transparent thermoelectric that can achieve high performance at low temperatures. The best result found in the literature corresponded to a zT of 1.12 at only 360 K, which is an outstanding result compared with the other materials listed in this review. Furthermore, this material is flexible and transparent, making it suitable for wearable devices.

From the reviewed literature, future trends in flexible TE materials are mainly oriented toward composites. The best performance, along with flexibility and printability, was achieved by combining different materials in synergy. In this context, MOFs and COFs are promising because their properties can be easily tuned. Furthermore, their organic nature makes them perfect candidates for green applications. Among inorganic materials, CuI is the most promising option owing to its high performance at low temperatures ($zT > 1$), nontoxicity, and abundance.

AUTHOR INFORMATION

Corresponding Authors

Francisco Molina-Lopez − *Department of Materials Engineering, KU Leuven, Leuven B-3001, Belgium;* orcid.org/0000-0002-4329-4059; Email: francisco.molinalopez@kuleuven.be

Almudena Rivadeneyra − *Department of Electronics and Computer Science, University of Granada, Granada 18071, Spain;* orcid.org/0000-0001-8133-1992; Email: arivadeneyra@ugr.es

Authors

Víctor Toral − *Department of Electronics and Computer Science, University of Granada, Granada 18071, Spain;* orcid.org/0000-0001-6720-3476

Sonia Gómez-Gijón − *Department of Electronics and Computer Science, University of Granada, Granada 18071, Spain*

Francisco J. Romero − *Department of Electronics and Computer Science, University of Granada, Granada 18071, Spain*

Diego P. Morales − *Department of Electronics and Computer Science, University of Granada, Granada 18071, Spain*

Encarnación Castillo − *Department of Electronics and Computer Science, University of Granada, Granada 18071, Spain*

Noel Rodríguez − *Department of Electronics and Computer Science, University of Granada, Granada 18071, Spain;* orcid.org/0000-0002-6032-6921

Sara Rojas − *Department of Inorganic Chemistry, University of Granada, Granada 18071, Spain;* orcid.org/0000-0002-7874-2122

Complete contact information is available at: https://pubs.acs.org/10.1021/acsaelm.4c00770

Notes

The authors declare no competing financial interest.

ACKNOWLEDGMENTS

This work was supported by the Junta de Andalucía, Consejería de Universidad, Investigación e Innovación, through Projects ProyExcel_00268 and P21_00105, by the Spanish Ministry of Sciences and Innovation through the National Projects CNS2022-135915 and TED2021-129949A-I00 and through the Ramón y Cajal Fellowships RYC2019-027457-I and RYC2021-0325. This project has received funding from the European Research Council under the

EU's Horizon 2020 research and innovation programme (Grant Agreement 948922) 3DALIGN.

■ REFERENCES

(1) Jouhara, H.; Żabnieńska-Góra, A.; Khordehgah, N.; Doraghi, Q.; Ahmad, L.; Norman, L.; Axcell, B.; Wrobel, L.; Dai, S. Thermoelectric generator (TEG) technologies and applications. *International Journal of Thermofluids* **2021**, *9*, No. 100063.

(2) Goodenough, J. B.; Kim, Y. Challenges for Rechargeable Li Batteries. *Chem. Mater.* **2010**, *22*, 587−603.

(3) Albatati, F.; Attar, A. Analytical and Experimental Study of Thermoelectric Generator (TEG) System for Automotive Exhaust Waste Heat Recovery. *Energies* **2021**, *14*, 204.

(4) Crane, D.; LaGrandeur, J.; Jovovic, V.; Ranalli, M.; Adldinger, M.; Poliquin, E.; Dean, J.; Kossakovski, D.; Mazar, B.; Maranville, C. TEG On-Vehicle Performance and Model Validation and What It Means for Further TEG Development. *J. Electron. Mater.* **2013**, *42*, 1582−1591.

(5) Yang, J.; Stabler, F. R. Automotive Applications of Thermoelectric Materials. *J. Electron. Mater.* **2009**, *38*, 1245−1251.

(6) Miao, Z.; Meng, X.; Liu, L. Improving the ability of thermoelectric generators to absorb industrial waste heat through three-dimensional structure optimization. *Appl. Therm. Eng.* **2023**, *228*, No. 120480.

(7) Ding, Z.; Du, C.; Long, W.; Cao, C.-F.; Liang, L.; Tang, L.-C.; Chen, G. Thermoelectrics and thermocells for fire warning applications. *Science Bulletin* **2023**, *68*, 3261−3277.

(8) Li, G.; Hu, Y.; Chen, J.; Liang, L.; Liu, Z.; Fu, J.; Du, C.; Chen, G. Thermoelectric and Photoelectric Dual Modulated Sensors for Human Internet of Things Application in Accurate Fire Recognition and Warning. *Adv. Funct. Mater.* **2023**, *33*, 2303861.

(9) Li, H.; Ding, Z.; Zhou, Q.; Chen, J.; Liu, Z.; Du, C.; Liang, L.; Chen, G. Harness High-Temperature Thermal Energy via Elastic Thermoelectric Aerogels. *Nano-Micro Lett.* **2024**, *16*, 1.

(10) Lv, H.; Liang, L.; Zhang, Y.; Deng, L.; Chen, Z.; Liu, Z.; Wang, H.; Chen, G. A flexible spring-shaped architecture with optimized thermal design for wearable thermoelectric energy harvesting. *Nano Energy* **2021**, *88*, No. 106260.

(11) Liang, L.; Wang, M.; Wang, X.; Peng, P.; Liu, Z.; Chen, G.; Sun, G. Initiating a Stretchable, Compressible, and Wearable Thermoelectric Generator by a Spiral Architecture with Ternary Nanocomposites for Efficient Heat Harvesting. *Adv. Funct. Mater.* **2022**, *32*, 15.

(12) Lu, X.; Xie, D.; Zhu, K.; Wei, S.; Mo, Z.; Du, C.; Liang, L.; Chen, G.; Liu, Z. Swift Assembly of Adaptive Thermocell Arrays for Device-Level Healable and Energy-Autonomous Motion Sensors. *Nano-Micro Lett.* **2023**, *15*, 1.

(13) Tian, R.; Liu, Y.; Koumoto, K.; Chen, J. Body Heat Powers Future Electronic Skins. *Joule* **2019**, *3*, 1399−1403.

(14) Du, C.; Cao, M.; Li, G.; Hu, Y.; Zhang, Y.; Liang, L.; Liu, Z.; Chen, G. Toward Precision Recognition of Complex Hand Motions: Wearable Thermoelectrics by Synergistic 2D Nanostructure Confinement and Controlled Reduction. *Adv. Funct. Mater.* **2022**, *32*, 36.

(15) Wang, D.; Shi, W.; Chen, J.; Xi, J.; Shuai, Z. Modeling thermoelectric transport in organic materials. *Phys. Chem. Chem. Phys.* **2012**, *14*, 16505.

(16) Korkosz, R. J.; Chasapis, T. C.; Lo, S.-h.; Doak, J. W.; Kim, Y. J.; Wu, C.-I.; Hatzikraniotis, E.; Hogan, T. P.; Seidman, D. N.; Wolverton, C.; Dravid, V. P.; Kanatzidis, M. G. High ZT in p-Type (PbTe)1−2x(PbSe)x(PbS)x Thermoelectric Materials. *J. Am. Chem. Soc.* **2014**, *136*, 3225−3237.

(17) Xiao, Y.; Zhao, L.-D. Charge and phonon transport in PbTe-based thermoelectric materials. *npj Quantum Materials* **2018**, *3*, 1.

(18) Tian, Y.; Florenciano, I.; Xia, H.; Li, Q.; Baysal, H. E.; Zhu, D.; Ramunni, E.; Meyers, S.; Yu, T.; Baert, K.; Hauffman, T.; Nider, S.; Göksel, B.; Molina-Lopez, F. Facile Fabrication of Flexible and High-Performing Thermoelectrics by Direct Laser Printing on Plastic Foil. *Adv. Mater.* **2024**, *36*, 2307945.

(19) Chen, Y.; Zhao, Y.; Liang, Z. Solution processed organic thermoelectrics: towards flexible thermoelectric modules. *Energy Environ. Sci.* **2015**, *8*, 401−422.

(20) Tian, Y.; Molina-Lopez, F. Boosting the performance of printed thermoelectric materials by inducing morphological anisotropy. *Nanoscale* **2021**, *13*, 5202−5215.

(21) Ju, D.; Kim, D.; Yook, H.; Han, J. W.; Cho, K. Controlling Electrostatic Interaction in PEDOT:PSS to Overcome Thermoelectric Tradeoff Relation. *Adv. Funct. Mater.* **2019**, *29*, 46.

(22) Kim, G.-H.; Shao, L.; Zhang, K.; Pipe, K. P. Engineered doping of organic semiconductors for enhanced thermoelectric efficiency. *Nat. Mater.* **2013**, *12*, 719−723.

(23) Li, C.; Luo, D.; Wang, T.; Shan, C.; Li, C.; Sun, K.; Kyaw, A. K. K.; Ouyang, J. Great Enhancement in the Seebeck Coefficient and Thermoelectric Properties of Solid PEDOT:PSS Films Through Molecular Energy Filtering by Zwitterions. *Small Structures* **2023**, *4*, 11.

(24) Vijayakumar, V.; Zhong, Y.; Untilova, V.; Bahri, M.; Herrmann, L.; Biniek, L.; Leclerc, N.; Brinkmann, M. Bringing Conducting Polymers to High Order: Toward Conductivities beyond 105 S cm-1 and Thermoelectric Power Factors of 2 mW m-1 K-2. *Adv. Energy Mater.* **2019**, *9*, 24.

(25) Yang, C.-Y.; Stoeckel, M.-A.; Ruoko, T.-P.; Wu, H.-Y.; Liu, X.; Kolhe, N. B.; Wu, Z.; Puttisong, Y.; Musumeci, C.; Massetti, M.; Sun, H.; Xu, K.; Tu, D.; Chen, W. M.; Woo, H. Y.; Fahlman, M.; Jenekhe, S. A.; Berggren, M.; Fabiano, S. A high-conductivity n-type polymeric ink for printed electronics. *Nat. Commun.* **2021**, *12*, 2354.

(26) Xu, K.; Sun, H.; Ruoko, T.-P.; Wang, G.; Kroon, R.; Kolhe, N. B.; Puttisong, Y.; Liu, X.; Fazzi, D.; Shibata, K.; Yang, C.-Y.; Sun, N.; Persson, G.; Yankovich, A. B.; Olsson, E.; Yoshida, H.; Chen, W. M.; Fahlman, M.; Kemerink, M.; Jenekhe, S. A.; Müller, C.; Berggren, M.; Fabiano, S. Ground-state electron transfer in all-polymer donor−acceptor heterojunctions. *Nat. Mater.* **2020**, *19*, 738−744.

(27) Tang, H.; Liang, Y.; Liu, C.; Hu, Z.; Deng, Y.; Guo, H.; Yu, Z.; Song, A.; Zhao, H.; Zhao, D.; Zhang, Y.; Guo, X.; Pei, J.; Ma, Y.; Cao, Y.; Huang, F. A solution-processed n-type conducting polymer with ultrahigh conductivity. *Nature* **2022**, *611*, 271−277.

(28) Liang, J.; Cui, R.; Zhang, X.; Koumoto, K.; Wan, C. Polymer/Carbon Composites with Versatile Interfacial Interactions for High Performance Carbon-Based Thermoelectrics: Principles and Applications. *Adv. Funct. Mater.* **2023**, *33*, 2208813.

(29) Li, D.; Gong, Y.; Chen, Y.; Lin, J.; Khan, Q.; Zhang, Y.; Li, Y.; Zhang, H.; Xie, H. Recent Progress of Two-Dimensional Thermoelectric Materials. *Nano-Micro Lett.* **2020**, *12*, 36.

(30) Ji, Z.; Li, Z.; Liu, L.; Zou, Y.; Di, C.; Zhu, D. Organic Thermoelectric Devices for Energy Harvesting and Sensing Applications. *Adv. Mater. Technol.* **2024**, *1*, 2302128.

(31) Deng, L.; Liu, Y.; Zhang, Y.; Wang, S.; Gao, P. Organic Thermoelectric Materials: Niche Harvester of Thermal Energy. *Adv. Funct. Mater.* **2023**, *33*, 2210770.

(32) Bao, Y.; Sun, Y.; Jiao, F.; Hu, W. Recent Advances in Multicomponent Organic Composite Thermoelectric Materials. *Adv. Electron. Mater.* **2023**, *9*, 5.

(33) Férey, G. Hybrid porous solids: past, present, future. *Chem. Soc. Rev.* **2008**, *37*, 191−214.

(34) Kitagawa, S.; Kitaura, R.; Noro, S. Functional Porous Coordination Polymers. *Angew. Chem., Int. Ed.* **2004**, *43*, 2334−2375.

(35) Furukawa, H.; Cordova, K. E.; O'Keeffe, M.; Yaghi, O. M. The Chemistry and Applications of Metal-Organic Frameworks. *Science* **2013**, *341*, 6149.

(36) Farha, O. K.; Eryazici, I.; Jeong, N. C.; Hauser, B. G.; Wilmer, C. E.; Sarjeant, A. A.; Snurr, R. Q.; Nguyen, S. T.; Yazaydın, A. O.; Hupp, J. T. Metal−Organic Framework Materials with Ultrahigh Surface Areas: Is the Sky the Limit? *J. Am. Chem. Soc.* **2012**, *134*, 15016−15021.

(37) Fan, Y.; Liu, Z.; Chen, G. Recent Progress in Designing Thermoelectric Metal−Organic Frameworks. *Small* **2021**, *17*, 2100505.

https://doi.org/10.1021/acsaelm.4c00770
ACS Appl. Electron. Mater. XXXX, XXX, XXX−XXX

(38) Lu, Y.; Young, D. J. Coordination polymers for n-type thermoelectric applications. *Dalton T.* **2020**, *49*, 7644−7657.
(39) Pajerowski, D. M.; Watanabe, T.; Yamamoto, T.; Einaga, Y. Electronic conductivity in Berlin green and Prussian blue. *Phys. Rev. B* **2011**, *83*, No. 153202.
(40) Gliemann, G.; Yersin, H. *Structure and Bonding (Berlin)*; Springer-Verlag, 2005; pp 87−153. .
(41) Lee, H.; Vashaee, D.; Wang, D. Z.; Dresselhaus, M. S.; Ren, Z. F.; Chen, G. Effects of nanoscale porosity on thermoelectric properties of SiGe. *J. Appl. Phys.* **2010**, *107*, 9.
(42) Park, J.; Hinckley, A. C.; Huang, Z.; Chen, G.; Yakovenko, A. A.; Zou, X.; Bao, Z. High Thermopower in a Zn-Based 3D Semiconductive Metal−Organic Framework. *J. Am. Chem. Soc.* **2020**, *142*, 20531−20535.
(43) Hmadeh, M.; Lu, Z.; Liu, Z.; Gándara, F.; Furukawa, H.; Wan, S.; Augustyn, V.; Chang, R.; Liao, L.; Zhou, F.; Perre, E.; Ozolins, V.; Suenaga, K.; Duan, X.; Dunn, B.; Yamamto, Y.; Terasaki, O.; Yaghi, O. M. New Porous Crystals of Extended Metal-Catecholates. *Chem. Mater.* **2012**, *24*, 3511−3513.
(44) Gonzalez-Juarez, M. d. L.; Flores, E.; Martin-Gonzalez, M.; Nandhakumar, I.; Bradshaw, D. Electrochemical deposition and thermoelectric characterisation of a semiconducting 2-D metal−organic framework thin film. *J. Mater. Chem. A* **2020**, *8*, 13197−13206.
(45) Lin, C.-C.; Huang, Y.-C.; Usman, M.; Chao, W.-H.; Lin, W.-K.; Luo, T.-T.; Whang, W.-T.; Chen, C.-H.; Lu, K.-L. Zr-MOF/Polyaniline Composite Films with Exceptional Seebeck Coefficient for Thermoelectric Material Applications. *ACS Appl. Mater. Interfaces* **2019**, *11*, 3400−3406.
(46) Xu, W.; Zhao, Y.; Wang, H.; Wang, H.; Pan, F.; Xu, R.; Hou, H. Postsynthetic-Modified PANI/MOF Composites with Tunable Thermoelectric and Photoelectric Properties. *Chemistry − A. European Journal* **2021**, *27*, 5011−5018.
(47) Qi, X.; Wang, Y.; Li, K.; Wang, J.; Zhang, H.-L.; Yu, C.; Wang, H. Enhanced electrical properties and restrained thermal transport in p- and n-type thermoelectric metal−organic framework hybrids. *J. Mater. Chem.A* **2021**, *9*, 310−319.
(48) Fan, Y.; Liu, Z.; Chen, G. Constructing flexible metal-organic framework/polymer/carbon nanotubes ternary composite films with enhanced thermoelectric properties for heat-to-electricity conversion. *Composites Communications* **2022**, *29*, No. 100997.
(49) Chen, Z.; Cui, Y.; Liang, L.; Wang, H.; Xu, W.; Zhang, Q.; Chen, G. Flexible film and thermoelectric device of single-walled carbon nanotube@conductive metal-organic framework composite. *Materials Today Nano* **2022**, *20*, No. 100276.
(50) Xue, Y.; Zhang, Z.; Zhang, Y.; Wang, X.; Li, L.; Wang, H.; Chen, G. Boosting thermoelectric performance by in situ growth of metal organic framework on carbon nanotube and subsequent annealing. *Carbon* **2020**, *157*, 324−329.
(51) Griggs, S.; Marks, A.; Bristow, H.; McCulloch, I. n-Type organic semiconducting polymers: stability limitations, design considerations and applications. *J. Mater. Chem. C* **2021**, *9*, 8099−8128.
(52) Moosavi, S. M.; Nandy, A.; Jablonka, K. M.; Ongari, D.; Janet, J. P.; Boyd, P. G.; Lee, Y.; Smit, B.; Kulik, H. J. Understanding the diversity of the metal-organic framework ecosystem. *Nat. Commun.* **2020**, *11*, 1.
(53) Park, Y.-W.; Heeger, A. J.; Druy, M. A.; MacDiarmid, A. G. Electrical transport in doped polyacetylene. *J. Chem. Phys.* **1980**, *73*, 946−957.
(54) Yang, Y.; Börjesson, K. Electroactive covalent organic frameworks: a new choice for organic electronics. *Trends in Chemistry* **2022**, *4*, 60−75.
(55) Chumakov, Y.; Aksakal, F.; Dimoglo, A.; Ata, A.; Palomares-Sánchez, S. A. First-Principles Study of Thermoelectric Properties of Covalent Organic Frameworks. *J. Electron. Mater.* **2016**, *45*, 3445−3452.
(56) Chumakov, Y.; Bayram, G. Theoretical Study of Thermoelectric Properties of Covalent Organic Frameworks with Slipped Arrangement. *J. Electron. Mater.* **2020**, *49*, 5498−5507.
(57) Pakhira, S.; Lucht, K. P.; Mendoza-Cortes, J. L. Iron Intercalation in Covalent−Organic Frameworks: A Promising Approach for Semiconductors. *J. Phys. Chem. C* **2017**, *121*, 21160−21170.
(58) Wang, L.; Dong, B.; Ge, R.; Jiang, F.; Xu, J. Fluorene-Based Two-Dimensional Covalent Organic Framework with Thermoelectric Properties through Doping. *ACS Appl. Mater. Interfaces* **2017**, *9*, 7108−7114.
(59) Wang, M.; Wang, M.; Lin, H.-H.; Ballabio, M.; Zhong, H.; Bonn, M.; Zhou, S.; Heine, T.; Cánovas, E.; Dong, R.; Feng, X. High-Mobility Semiconducting Two-Dimensional Conjugated Covalent Organic Frameworks with p-Type Doping. *J. Am. Chem. Soc.* **2020**, *142*, 21622−21627.
(60) Jin, E.; Geng, K.; Fu, S.; Yang, S.; Kanlayakan, N.; Addicoat, M. A.; Kungwan, N.; Geurs, J.; Xu, H.; Bonn, M.; Wang, H. I.; Smet, J.; Kowalczyk, T.; Jiang, D. Exceptional electron conduction in two-dimensional covalent organic frameworks. *Chem.* **2021**, *7*, 3309−3324.
(61) Xie, J.; Han, M.; Zeng, X.; Mao, D.; Li, H.; Zeng, X.; Liu, R.; Ren, L.; Sun, R.; Xu, J. Flexible pCu_2Se−nAg_2Se thermoelectric devices via in situ conversion from printed Cu patterns. *Chem. Eng. J.* **2022**, *435*, No. 135172.
(62) Mallick, M. M.; Sarbajna, A.; Rösch, A. G.; Franke, L.; Geßwein, H.; Eggeler, Y. M.; Lemmer, U. Ultra-flexible β−$Cu_{2-\delta}Se$-based p-type printed thermoelectric films. *Appl. Mater. Today* **2022**, *26*, No. 101269.
(63) Mallick, M. M.; Franke, L.; Rösch, A. G.; Geßwein, H.; Eggeler, Y. M.; Lemmer, U. Photonic Curing Enables Ultrarapid Processing of Highly Conducting β−$Cu_{2-\delta}Se$ Printed Thermoelectric Films in Less Than 10 ms. *ACS Omega* **2022**, *7*, 10695−10700.
(64) Qin, J.; Du, Y.; Meng, Q.; Ke, Q. Flexible thermoelectric Cu−Se nanowire/methyl cellulose composite films prepared via screen printing technology. *Composites Communications* **2023**, *38*, No. 101467.
(65) Liu, W.-D.; Yang, L.; Chen, Z.-G.; Zou, J. Promising and Eco-Friendly CU2X-Based Thermoelectric Materials: Progress and Applications. *Adv. Mater.* **2020**, *32*, 1905703.
(66) Burton, M. R.; Mehraban, S.; McGettrick, J.; Watson, T.; Lavery, N. P.; Carnie, M. J. Earth abundant, non-toxic, 3D printed Cu2−xS with high thermoelectric figure of merit. *J. Mater. Chem. A* **2019**, *7*, 25586−25592.
(67) He, Y.; Day, T.; Zhang, T.; Liu, H.; Shi, X.; Chen, L.; Snyder, G. J. High Thermoelectric Performance in Non-Toxic Earth-Abundant Copper Sulfide. *Adv. Mater.* **2014**, *26*, 3974−3978.
(68) Yue, Z.; Zhou, W.; Ji, X.; Wang, Y.; Guo, F. Thermoelectric performance of hydrothermally synthesized micro/nano Cu2−xS. *Chem. Eng. J.* **2022**, *449*, No. 137748.
(69) Zhang, Y.; Xing, C.; Liu, Y.; Spadaro, M. C.; Wang, X.; Li, M.; Xiao, K.; Zhang, T.; Guardia, P.; Lim, K. H.; Moghaddam, A. O.; Llorca, J.; Arbiol, J.; Ibáñez, M.; Cabot, A. Doping-mediated stabilization of copper vacancies to promote thermoelectric properties of Cu2−xS. *Nano Energy* **2021**, *85*, No. 105991.
(70) Zhao, J.; Zhao, X.; Guo, R.; Zhao, Y.; Yang, C.; Zhang, L.; Liu, D.; Ren, Y. Preparation and Characterization of Screen-Printed Cu2S/PEDOT:PSS Hybrid Films for Flexible Thermoelectric Power Generator. *Nanomaterials* **2022**, *12*, 2430.
(71) Yang, C.; Souchay, D.; Kneiß, M.; Bogner, M.; Wei, H. M.; Lorenz, M.; Oeckler, O.; Benstetter, G.; Fu, Y. Q.; Grundmann, M. Transparent flexible thermoelectric material based on non-toxic earth-abundant p-type copper iodide thin film. *Nat. Commun.* **2017**, *8*, 16076.
(72) Morais Faustino, B. M.; Gomes, D.; Faria, J.; Juntunen, T.; Gaspar, G.; Bianchi, C.; Almeida, A.; Marques, A.; Tittonen, I.; Ferreira, I. CuI p-type thin films for highly transparent thermoelectric p-n modules. *Sci. Rep.* **2018**, *8*, 6867.

https://doi.org/10.1021/acsaelm.4c00770
ACS Appl. Electron. Mater. XXXX, XXX, XXX−XXX

(73) Almasoudi, M.; Saeed, A.; Salah, N.; Alshahrie, A.; Hasan, P. M. Z.; Melaibari, A.; Koumoto, K. CuI: A Promising Halide for Thermoelectric Applications below 373 K. *ACS Appl. Energy Mater.* **2022**, *5*, 10177−10186.

(74) Salah, N.; Abusorrah, A. M.; Salah, Y. N.; Almasoudi, M.; Baghdadi, N.; Alshahri, A.; Koumoto, K. Effective dopants for CuI single nanocrystals as a promising room temperature thermoelectric material. *Ceram. Int.* **2020**, *46*, 27244−27253.

(75) Maji, T.; Rousti, A. M.; Kazi, A. P.; Drew, C.; Kumar, J.; Christodouleas, D. C. Wearable Thermoelectric Devices Based on Three-Dimensional PEDOT:Tosylate/CuI Paper Composites. *ACS Appl. Mater. Interfaces* **2021**, *13*, 46919−46926.

(76) Naguib, M.; Kurtoglu, M.; Presser, V.; Lu, J.; Niu, J.; Heon, M.; Hultman, L.; Gogotsi, Y.; Barsoum, M. W. Two-Dimensional Nanocrystals Produced by Exfoliation of Ti3AlC2. *Adv. Mater.* **2011**, *23*, 4248−4253.

(77) Alnoor, H.; Elsukova, A.; Palisaitis, J.; Persson, I.; Tseng, E.; Lu, J.; Hultman, L.; Persson, P. Exploring MXenes and their MAX phase precursors by electron microscopy. *Materials Today Advances* **2021**, *9*, No. 100123.

(78) Gogotsi, Y.; Anasori, B. The Rise of MXenes. *ACS Nano* **2019**, *13*, 8491−8494.

(79) Goossens, N.; Lambrinou, K.; Tunca, B.; Kotasthane, V.; Rodríguez González, M. C.; Bazylevska, A.; Persson, P. O. A.; De Feyter, S.; Radovic, M.; Molina-Lopez, F.; Vleugels, J. Upscaled Synthesis Protocol for Phase-Pure, Colloidally Stable MXenes with Long Shelf Lives. *Small Methods* **2024**, *8*, 1.

(80) Huang, D.; Kim, H.; Zou, G.; Xu, X.; Zhu, Y.; Ahmad, K.; Almutairi, Z. A.; Alshareef, H. N. All-MXene thermoelectric nanogenerator. *Materials Today. Energy* **2022**, *29*, No. 101129.

(81) Liu, P.; Ding, W.; Liu, J.; Shen, L.; Jiang, F.; Liu, P.; Zhu, Z.; Zhang, G.; Liu, C.; Xu, J. Surface termination modification on high-conductivity MXene film for energy conversion. *J. Alloy. Compd.* **2020**, *829*, No. 154634.

(82) Wang, Z.; Chen, M.; Cao, Z.; Liang, J.; Liu, Z.; Xuan, Y.; Pan, L.; Razeeb, K. M.; Wang, Y.; Wan, C.; Zong, P.-a. MXene Nanosheet/Organics Superlattice for Flexible Thermoelectrics. *ACS Appl. Nano Mater.* **2022**, *5*, 16872−16883.

(83) Wang, Z.; Zhang, C.; Zhang, J.; liang, J.; Liu, Z.; Hang, F.; Xuan, Y.; Wang, X.; Chen, M.; Tang, S.; Zong, P.-a. Construction of an MXene/Organic Superlattice for Flexible Thermoelectric Energy Conversion. *ACS Appl. Energy Mater.* **2022**, *5*, 11351−11361.

(84) Sarikurt, S.; Çakır, D.; Keçeli, M.; Sevik, C. The influence of surface functionalization on thermal transport and thermoelectric properties of MXene monolayers. *Nanoscale* **2018**, *10*, 8859−8868.

(85) Guo, Y.; Du, J.; Hu, M.; Wei, B.; Su, T.; Zhou, A. Improve thermoelectric performance of Bi2Te3 by incorporation of Mo2C MXene with N-type conductivity. *J. Mater. Sci. Mater. Electron.* **2023**, *34*, 685.

(86) Zhang, D.; Cao, Y.; Hui, Y.; Cai, J.; Ji, J.; Yin, H.; Zhang, M.; Xu, J.; Zhang, Q. Enhancements of thermoelectric performance in n-type Bi2Te3-based nanocomposites through incorporating 2D Mxenes. *J. Eur. Ceram. Soc.* **2022**, *42*, 4587−4593.

(87) Lu, X.; Zhang, Q.; Liao, J.; Chen, H.; Fan, Y.; Xing, J.; Gu, S.; Huang, J.; Ma, J.; Wang, J.; Wang, L.; Jiang, W. High-Efficiency Thermoelectric Power Generation Enabled by Homogeneous Incorporation of MXene in (Bi,Sb)2Te3Matrix. *Adv. Energy Mater.* **2020**, *10*, 1902986.

(88) Fan, S.; Sun, T.; Jiang, M.; Gu, S.; Wang, L.; Jiang, W. Enhanced thermoelectric performance of MXene/GeTe through a facile freeze-drying method. *J. Alloy. Compd.* **2023**, *948*, No. 169807.

(89) Zhang, H.; Chen, Y.; Liu, X.; Wang, H.; Niu, C.; Zheng, S.; Zhang, B.; Lu, X.; Wang, G.; Han, G.; Zhou, X. Enhancing the thermoelectric performance of solution-synthesized SnSe-based materials via incorporating Ti3C2T MXene. *Materials Today Energy* **2022**, *30*, No. 101137.

(90) Jiang, X.-P.; Tian, B.-Z.; Sun, Q.; Li, X.-L.; Chen, J.; Tang, J.; Zhang, P.; Yang, L.; Chen, Z.-G. Enhanced thermoelectric performance in MXene/SnTe nanocomposites synthesized via a facile one-step solvothermal method. *J. Solid State Chem.* **2021**, *304*, No. 122605.

(91) Yan, L.; Luo, X.; Yang, R.; Dai, F.; Zhu, D.; Bai, J.; Zhang, L.; Lei, H. Highly Thermoelectric ZnO@MXene (Ti3C2Txi) Composite Films Grown by Atomic Layer Deposition. *ACS Appl. Mater. Interfaces* **2022**, *14*, 34562−34570.

(92) Karthikeyan, V.; Theja, V. C. S.; De Souza, M. M.; Roy, V. A. L. Hierarchically Interlaced 2D Copper Iodide/MXene Composite for High Thermoelectric Performance. *Physica Rapid Res. Lett.* **2022**, *16*, 2100419.

(93) Wei, J.; Wu, D.; Liu, C.; Zhong, F.; Cao, G.; Li, B.; Gao, C.; Wang, L. Free-standing p-Type SWCNT/MXene composite films with low thermal conductivity and enhanced thermoelectric performance. *Chem. Eng. J.* **2022**, *439*, No. 135706.

(94) Ding, W.; Liu, P.; Bai, Z.; Wang, Y.; Liu, G.; Jiang, Q.; Jiang, F.; Liu, P.; Liu, C.; Xu, J. Constructing Layered MXene/CNTs Composite Film with 2D−3D Sandwich Structure for High Thermoelectric Performance. *Adv. Mater. Interfaces* **2020**, *7*, 2001340.

(95) Guan, X.; Feng, W.; Wang, X.; Venkatesh, R.; Ouyang, J. Significant Enhancement in the Seebeck Coefficient and Power Factor of p-Type Poly(3,4-ethylenedioxythiophene):Poly(styrenesulfonate) through the Incorporation of n-Type MXene. *ACS Appl. Mater. Interfaces* **2020**, *12*, 13013−13020.

(96) Dixit, P.; Jana, S. S.; Maiti, T. Enhanced Thermoelectric Performance of Rare-Earth-Free n-Type Oxide Perovskite Composite with Graphene Analogous 2D MXene. *Small* **2023**, *19*, 2206710.

(97) Huang, H. H.; Fan, X.; Singh, D. J.; Zheng, W. T. Recent progress of TMD nanomaterials: phase transitions and applications. *Nanoscale* **2020**, *12*, 1247−1268.

(98) Pallecchi, I.; Manca, N.; Patil, B.; Pellegrino, L.; Marré, D. Review on thermoelectric properties of transition metal dichalcogenides. *Nano Futures* **2020**, *4*, No. 032008.

(99) Chen, K.-X.; Wang, X.-M.; Mo, D.-C.; Lyu, S.-S. Thermoelectric Properties of Transition Metal Dichalcogenides: From Monolayers to Nanotubes. *J. Phys. Chem. C* **2015**, *119*, 26706−26711.

(100) Ding, Z.; Yang, S.-W.; Wu, G.; Yang, X. Geometry and Greatly Enhanced Thermoelectric Performance of Monolayer MXY Transition-Metal Dichalcogenide: MoSTe as an Example. *Physica Rapid Res. Lett.* **2021**, *15*, 2100166.

(101) Ouyang, Y.; Xie, Y.; Zhang, Z.; Peng, Q.; Chen, Y. Very high thermoelectric figure of merit found in hybrid transition-metal-dichalcogenides. *J. Appl. Phys.* **2016**, *120*, 235109.

(102) Ghosh, K.; Singisetti, U. Thermoelectric transport coefficients in mono-layer MoS2 and WSe2: Role of substrate, interface phonons, plasmon, and dynamic screening. *J. Appl. Phys.* **2015**, *118*, 135711.

(103) Deng, S.; Li, L.; Guy, O. J.; Zhang, Y. Enhanced thermoelectric performance of monolayer MoSSe, bilayer MoSSe and graphene/MoSSe heterogeneous nanoribbons. *Phys. Chem. Chem. Phys.* **2019**, *21*, 18161−18169.

(104) Purwitasari, W.; Villaos, R. A. B.; Verzola, I. M. R.; Sufyan, A.; Huang, Z.-Q.; Hsu, C.-H.; Chuang, F.-C. High Thermoelectric Performance in 2D Technetium Dichalcogenides TcX2 (X = S, Se, or Te). *ACS Appl. Energy Mater.* **2022**, *5*, 8650−8657.

(105) Patil, B.; Bernini, C.; Marré, D.; Pellegrino, L.; Pallecchi, I. Ink-jet printing and drop-casting deposition of 2H-phase SnSe2 and WSe2 nanoflake assemblies for thermoelectric applications. *Nanotechnology* **2022**, *33*, No. 035302.

(106) Lee, W.-Y.; Kang, M.-S.; Kim, G.-S.; Choi, J. W.; Park, N.-W.; Sim, Y.; Kim, Y.-H.; Seong, M.-J.; Yoon, Y.-G.; Saitoh, E.; Lee, S.-K. Interface-Induced Seebeck Effect in PtSe2/PtSe2 van der Waals Homostructures. *ACS Nano* **2022**, *16*, 3404−3416.

(107) Nghia, D. X.; Baek, J. J.; Oh, J. Y.; Lee, T. I. Deformable thermoelectric sponge based on layer-by-layer self-assembled transition metal dichalcogenide nanosheets for powering electronic skin. *Ceram. Int.* **2023**, *49*, 9307−9315.

(108) Zeng, Z.; Yin, Z.; Huang, X.; Li, H.; He, Q.; Lu, G.; Boey, F.; Zhang, H. Single-Layer Semiconducting Nanosheets: High-Yield Preparation and Device Fabrication. *Angew. Chem., Int. Ed.* **2011**, *50*, 11093−11097.

https://doi.org/10.1021/acsaelm.4c00770
ACS Appl. Electron. Mater. XXXX, XXX, XXX−XXX

(109) Zhang, R.-z.; Wan, C.-l.; Wang, Y.-f.; Koumoto, K. Titanium sulphene: two-dimensional confinement of electrons and phonons giving rise to improved thermoelectric performance. *Phys. Chem. Chem. Phys.* **2012**, *14*, 15641.

(110) Li, G.; Yao, K.; Gao, G. Strain-induced enhancement of thermoelectric performance of TiS2monolayer based on first-principles phonon and electron band structures. *Nanotechnology* **2018**, *29*, No. 015204.

(111) Salah, N.; Abdullahi, S.; Baghdadi, N.; Alshahrie, A.; Koumoto, K. High Thermoelectric Power Generation below Room Temperature by TiS2 Compact Pellet. *ACS Applied Electronic Materials* **2024**, *6*, 2839−2850.

(112) Gu, Y.; Song, K.; Hu, X.; Chen, C.; Pan, L.; Lu, C.; Shen, X.; Koumoto, K.; Wang, Y. Realization of an Ultrahigh Power Factor and Enhanced Thermoelectric Performance in TiS2 via Microstructural Texture Engineering. *ACS Appl. Mater. Interfaces* **2020**, *12*, 41687−41695.

(113) Wang, T.; Liu, C.; Jiang, F.; Xu, Z.; Wang, X.; Li, X.; Li, C.; Xu, J.; Yang, X. Solution-processed two-dimensional layered heterostructure thin-film with optimized thermoelectric performance. *Phys. Chem. Chem. Phys.* **2017**, *19*, 17560−17567.

(114) Li, X.; Wang, T.; Jiang, F.; Liu, J.; Liu, P.; Liu, G.; Xu, J.; Liu, C.; Jiang, Q. Optimizing thermoelectric performance of MoS2 films by spontaneous noble metal nanoparticles decoration. *J. Alloy. Compd.* **2019**, *781*, 744−750.

(115) Xin, N.; Tang, G.; Lan, T.; Li, Y.; Kou, J.; Zhang, M.; Zhao, X.; Nie, Y. Improving the thermoelectric performance of Cu-doped MoS2 film by band structure modification and microstructural regulation. *Appl. Surf. Sci.* **2023**, *611*, No. 155611.

(116) Yang, Y.; He, D.; Zhou, Y.; Wen, S.; Huang, H. Electronic and surface modulation of 2D MoS2 nanosheets for an enhancement on flexible thermoelectric property. *Nanotechnology* **2023**, *34*, 195401.

(117) Wan, C.; Gu, X.; Dang, F.; Itoh, T.; Wang, Y.; Sasaki, H.; Kondo, M.; Koga, K.; Yabuki, K.; Snyder, G. J.; Yang, R.; Koumoto, K. Flexible n-type thermoelectric materials by organic intercalation of layered transition metal dichalcogenide TiS2. *Nat. Mater.* **2015**, *14*, 622−627.

(118) Wan, C.; Tian, R.; Kondou, M.; Yang, R.; Zong, P.; Koumoto, K. Ultrahigh thermoelectric power factor in flexible hybrid inorganic-organic superlattice. *Nat. Commun.* **2017**, *8*, 1.

(119) Tian, R.; Wan, C.; Wang, Y.; Wei, Q.; Ishida, T.; Yamamoto, A.; Tsuruta, A.; Shin, W.; Li, S.; Koumoto, K. A solution-processed TiS2/organic hybrid superlattice film towards flexible thermoelectric devices. *J. Mater. Chem.A* **2017**, *5*, 564−570.

(120) Wang, L.; Zhang, Z.; Geng, L.; Yuan, T.; Liu, Y.; Guo, J.; Fang, L.; Qiu, J.; Wang, S. Solution-printable fullerene/TiS2 organic/inorganic hybrids for high-performance flexible n-type thermoelectrics. *Energy Environ. Sci.* **2018**, *11*, 1307−1317.

(121) Wang, S.; Yang, X.; Hou, L.; Cui, X.; Zheng, X.; Zheng, J. Organic covalent modification to improve thermoelectric properties of TaS2. *Nat. Commun.* **2022**, *13*, 4401.

(122) Ling, X.; Wang, H.; Huang, S.; Xia, F.; Dresselhaus, M. S. The renaissance of black phosphorus. *Proc. Natl. Acad. Sci. U. S. A.* **2015**, *112*, 4523−4530.

(123) Zhang, Y.; Wang, J.; Liu, Q.; Gu, S.; Sun, Z.; Chu, P. K.; Yu, X. The electrical, thermal, and thermoelectric properties of black phosphorus. *APL Mater.* **2020**, *8*, 120903.

(124) Peng, B.; Zhang, H.; Shao, H.; Xu, K.; Ni, G.; Li, J.; Zhu, H.; Soukoulis, C. M. Chemical intuition for high thermoelectric performance in monolayer black phosphorus, α-arsenene and aW-antimonene. *J. Mater. Chem.A* **2018**, *6*, 2018−2033.

(125) Cui, Y.-F.; Duan, S.; Chen, X.; Yang, M.-M.; Yang, B.-C.; Yi, W.-C.; Liu, X.-B. Prediction of enhanced thermoelectric performance in two-dimensional black phosphorus nanosheets. *Vacuum* **2021**, *183*, No. 109790.

(126) Flores, E.; Ares, J. R.; Castellanos-Gomez, A.; Barawi, M.; Ferrer, I. J.; Sánchez, C. Thermoelectric power of bulk black-phosphorus. *Appl. Phys. Lett.* **2015**, *106*, No. 022102.

(127) Zeng, Q.; Sun, B.; Du, K.; Zhao, W.; Yu, P.; Zhu, C.; Xia, J.; Chen, Y.; Cao, X.; Yan, Q.; Shen, Z.; Yu, T.; Long, Y.; Koh, Y. K.; Liu, Z. Highly anisotropic thermoelectric properties of black phosphorus crystals. *2D Mater.* **2019**, *6*, No. 045009.

(128) Song, J.; Duan, S.; Chen, X.; Li, X.; Yang, B.; Liu, X. Synthesis of Highly Stable One-Dimensional Black Phosphorus/h-BN Heterostructures: A Novel Flexible Electronic Platform. *Chin. Phys. Lett.* **2020**, *37*, No. 076203.

(129) Novak, T. G.; Shin, H.; Kim, J.; Kim, K.; Azam, A.; Nguyen, C. V.; Park, S. H.; Song, J. Y.; Jeon, S. Low-Cost Black Phosphorus Nanofillers for Improved Thermoelectric Performance in PEDOT:PSS Composite Films. *ACS Appl. Mater. Interfaces* **2018**, *10*, 17957−17962.

https://doi.org/10.1021/acsaelm.4c00770
ACS Appl. Electron. Mater. XXXX, XXX, XXX−XXX